ISSN 0024-4902, Lithology and Mineral Resources, 2024, Vol. 59, No. 4, pp. 357–380. © Pleiades Publishing, Ltd., 2024.

Lithogeochemistry of Upper Precambrian Terrigenous Rocks in Belarus: Communication 1. Bulk Chemical Composition, General Features, and Anomalies

A. V. Maslov[a, *], O. Yu. Melnichuk[b], A. B. Kuznetsov[c], and V. N. Podkovyrov[c]

[a] *Geological Institute, Russian Academy of Sciences, Moscow, 119017 Russia*

[b] *Zavaritsky Institute of Geology and Geochemistry, Ural Branch, Russian Academy of Sciences, Yekaterinburg, 620110 Russia*

[c] *Institute of Precambrian Geology and Geochronology, Russian Academy of Sciences, St. Petersburg, 199034 Russia*

**e-mail: amas2004@mail.ru*

Received January 9, 2024; revised February 7, 2024; accepted February 15, 2024

Abstract—The first of two communications is devoted to the study of lithogeochemical features of the pilot collection of Upper Precambrian sandstone and siltstone samples taken from four boreholes: Bogushevskaya 1, Bykhovskaya, Lepel 1, and Kormyanskaya (Belarus). This article analyzes the general features of their bulk chemical composition and shows the possibilities and limitations for further reconstructions. It has been established that Riphean and Vendian rocks included in the pilot collection, visually identified as sandstones, are actually quartz, feldspar–quartz, and arkosic varieties with different cement types. In terms of geochemical characteristics, the Vendian "siltstones" correspond to the coarse- and fine-grained siltstones and, to a greater extent, mudstones with a predominance of illite, as well as various admixtures of berthierine, kaolinite, and smectite. Based on the comparison of enrichment factor (EF) of the trace element, these rocks are marked by several dissimilarities related to both variations in the source rock composition and sedimentary environment. Data points of the samples on the Zr/Sc–Th/Sc diagram indicate that all of the studied Riphean and Vendian rocks are dominated by the first sedimentation cycle material, suggesting that the lithogeochemical characteristics of the pilot collection rocks quite correctly reflect similar features of the source rock complexes. Therefore, they can be used to reconstruct the paleogeodynamic and paleoclimatic factors that controlled the accumulation of Riphean and Vendian sedimentary sequences in Belarus.

Keywords: Riphean, Vendian, sandstones, siltstones, claystones, lithogeochemical features, East European Platform, Belarus

DOI: 10.1134/S0024490224700627

INTRODUCTION

The Upper Precambrian sedimentary sequences, widespread in the Republic of Belarus in the western East European Platform (EEP), belong to both Riphean and Vendian (*Geologiya* ..., 2001; Kuzmenkova et al., 2018, 2019a, 2019b; Laptsevich et al., 2023; Makhnach, 1966; Makhnach et al., 1975 and others; *Stratigraficheskie* ..., 2010; Streltsova et al., 2023). As in the stratotype section in the Southern Urals, the Riphean section in Belarus is divided into three (Lower, Middle, and Upper Riphean) erathems. Its rocks overlie the EEP crystalline basement with a major stratigraphic hiatus. They are also overlain unconformably by the glacial cover of the Vilchitsy Group, but by the volcanogenic and volcanosedimentary rocks of the Vendian Volyn Formation if the glacial cover is absent.

Here, the Bobruisk Group belongs to the Lower Riphean; the Sherovichi Group, presumably, to the Middle Riphean; and the Belarus Group, to the Middle–Upper Riphean (*Stratigraficheskie* ..., 2010). These stratons, as and the Vendian deposits were accumulated in a number of large, successively replacing each other, paleostructures (*Geologiya* ..., 2001; Kuzmenkova et al., 2018, 2019a, 2019b; Makhnach et al., 1976; Streltsova et al., 2023): Volyn–Orsha paleotrough/paleoaulacogen (Sherovichi, Belarus, and Vilchitsy groups), large magmatic Volyn–Brest province, Kobrin–Mogilev (Volyn Group), and Kobrin–Polotsk paleotroughs (Valdai Group).

When evaluating the presented material and conclusions thereafter, we should bear in mind that the geochemical studies of sedimentary (Upper Precambrian included) rocks in Belarus have a long history (Bordon, 1977 and others; Kuzmenkova et al., 2018 and references therein; Makhnach et al., 1982 et al., Yudovich, 2007). Without dwelling on it in detail, let us only note the following point: according to (Bordon, 1977), the Lower Vendian sandy–silty, clayey, and tillite-type rocks of the Glusk Formation have a

low (below-Clarke) background content of trace elements. Their distribution is irregular, indicating the predominance of physical weathering in the provenance. The Gluskian runoff areas were composed of acid and, possibly, intermediate rocks. The sandy–silty rocks of the Upper Vendian Kotlin Formation have a higher (above-Clarke) content of Ti, Ga, Y, and Ba. The distribution of trace elements corresponds to the transitional subtype in the classification by N.M. Strakhov. Hence, not only physical, but also chemical weathering took place in the provenance.

The present and next communication complement to some extent and expand the conclusions made earlier by Belarusian colleagues. These works are devoted to the studies of lithogeochemical characteristics of the pilot collection of sandstone and fine-grained clastic rock (fine-grained clayey siltstone and claystone) samples taken from the Upper Precambrian rock sections (Belarus, Vilchitsy, Volyn, and Valdai groups) in Belarus. They scrutinized and significantly expanded the conclusions on the composition and evolution of rocks in the fine-grained aluminosiliciclastic sources reported in (Maslov et al., 2024) when analyzing the database for terrigenous rocks (mudstones) of the Volyn, Redkino, and Kotlin regional stages, as well as for Lower Cambrian rocks of the Belarus and Volyn stages in (Jewuła et al., 2022). Additionally, these works address the paleogeodynamic, paleoclimatic, and paleogeographic conditions of the formation of several Riphean and Vendian sedimentary sequences.

LITHOSTRATIGRAPHY AND COMPOSITION OF RIPHEAN AND VENDIAN SEDIMENTARY SEQUENCES

This section describes mainly lithostratigraphic units of the Belarus, Vilchitsy, Volyn, and Valdai groups represented in Belarus, where sandstones and siltstones were sampled (Fig. 1). The Belarus Group unites the Rogachev, Rudnya, Pinsk (stratigraphic analog of the latter unit), and Orsha formations. The age of all above-listed lithostratigraphic units is considered as Middle Riphean (Kuzmenkova et al., 2019a, 2019b; *Stratigraficheskie* ..., 2010; Streltsova et al., 2023). According to a recent publication on the age of clastic zircon, the Orsha and Pinsk formations were accumulated 1.32–1.00 Ga ago (Paszkowski et al., 2019). The Lapichi Formation, which terminates the section, belongs to the Upper Riphean estimated at ~710 Ma (Środoń et al., 2022).

The Rogachev Formation (40 m thick), composed of the fine-, medium-, and varigrained arkosic sandstones, lies on rocks of the crystalline basement and, in some places, on sandstones of the Middle? Riphean Bortniks Formation (Sherovichi Group) (*Geologiya* ..., 2001; Kuzmenkova et al., 2019a; *Stratigraficheskie* ..., 2010; Streltsova et al., 2023). The Rudnya Formation (300 m) is represented mainly by the oligomictic and almost pure quartz-rich (in the upper part) red-colored sandstones, with rare interlayers and frequent "rolls" of siltstones and clays. In the lower part of the formation (over 10–25 m from the base), one can see variable (in grain size) alternations of feldspar–quartz sandstones (including the coarse-grained variety with gravel and pebble) and the basal conglomerate or clay breccia at the base (*Geologiya* ..., 2001). The Pinsk Formation (up to 460 m thick) unites the red-colored oligomictic and mesomictic silty sandstones and sandy siltstones. This formation also includes thin (from 0.*n* to 5–10 m) members of alternating laminated siltstones, claystones, and sandstones. Interlayers of the clayey varieties show desiccation cracks. The Orsha Formation (up to 620 m) is almost completely composed of the red-colored fine- and medium-grained oligomictic and quartz-rich sandstones. At the formation bottom (over 7–10 m from the base), a gravel–pebble conglomerate layer lies on the Rudnya Formation (*Geologiya* ..., 2001). Along the periphery of the eponymous depression, the Orsha Formation overlies the weathering crust developed after the crystalline basement. The Lapichi Formation (up to 82 m) unconformably overlies the red-colored sandstones and mudstones of the Pinsk (more rarely, Orsha) Formation and is overlain with erosion by the Vilchitsy Group. The Orsha Formation unites the stromatolitic and catagraphic dolomites (with the sandy–silty and ferruginous–clayey admixture), sandstones (with the clay–dolomite cement), clayey and sandy siltstones, polymictic conglomerates, as well as conglobreccias and dolomitic breccias (*Geologiya* ..., 2001; Środoń et al., 2022; Streltsova et al., 2023). Sandstones of the Bortniks and Rudnya formations in the Volyn–Orsha trough were accumulated no later than 1 Ga ago, as is evident from the U–Th–Pb age of detrital zircon (Zaitseva et al., 2023). Thus, the age of the Sherovichi and Belarus groups, previously considered as Middle Riphean, is now defined as Late Riphean.

New information about the petrography and geochemistry of the Riphean and Vendian lithostratigraphic units in Belarus was obtained by studying samples of the Rudnya, Orsha, and Glusk formations recovered in 2017 by the parametric borehole Bykhovskaya at the Orsha depression/Zhlobin saddle junction (Kuzmenkova et al., 2018). In borehole Bykhovskaya, the Rudnya Formation is dominated by the polymictic sandstones with poorly sorted/rounded fragments of quartz, feldspar, quartzite, and granite with hydromica, smectite, hematite, and less common kaolinite. The oligomictic sandstones appear in the upper part. At the same time, the hydrolyzate module (HM) is 0.32–0.13 in polymictic sandstones of the Rudnya Formation and 0.06 in the oligomictic variety (Kuzmenkova et al., 2018). The Vendian Orsha Formation is represented by almost monomineral quartz sandstones with HM = 0.07. The Glusk Formation in borehole Bykhovskaya is represented by moraine deposits of red tillites of predominantly sand dimen-

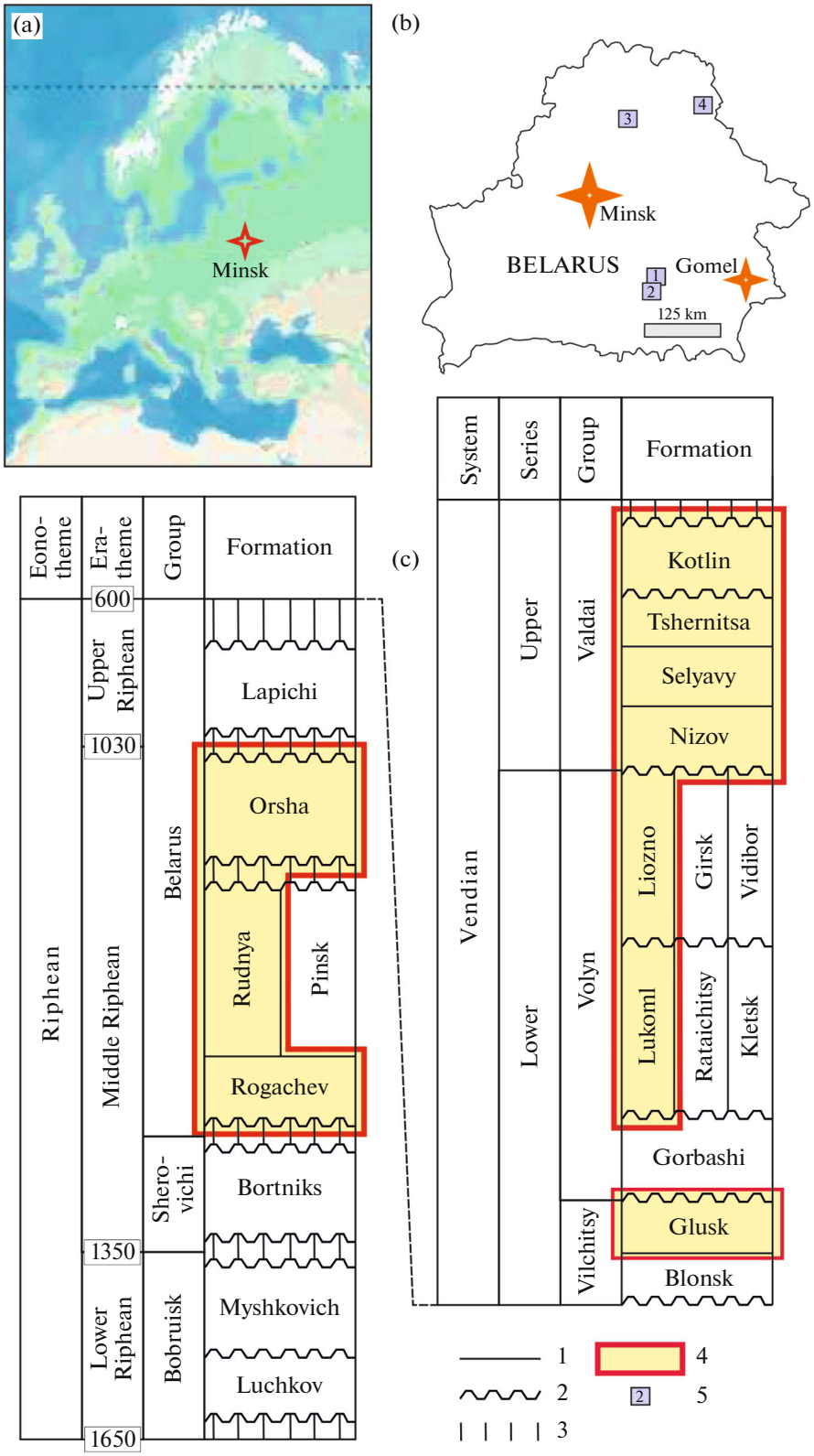

Fig. 1. Schematic location of the studied boreholes (a) and summary Upper Precambrian stratigraphic column in Belarus (b). Modified after (*Stratigraficheskie* ..., 2010). The geographic base is adopted from https://yandex.ru/maps/?ll=166.992700%2C21.912809&z=2. (1–3) relationship between stratons: (1) conformable, (2) unconformable, (3) proven stratigraphic hiatuses; (4) sampled section intervals; (5) boreholes: (1) Bykhovskaya, (2) Kormyanskaya, (3) Lepel 1, (4) Bogushevskaya 1. The age boundary of large stratigraphic subdivisions (in Ma) given according to (*Stratigraficheskie* ..., 2010).

sion with quartzite pebbles and boulders (HM = 0.11), fluvioglacial deposits with the oligomictic quartz-rich sands and sandstones of variable sorting degree (HM = 0.04–0.19), and lacustrine-glacial deposits of red-brown banded kaolinite–hydromica clays (HM = 0.58). The mineral–chemical composition of sandstones and tillites of the Glusk Formation is similar to that in the underlying sandstones of the Rudnya and Orsha formations, indicating a significant degree of Riphean rock assimilation by the Vendian glacier (Kuzmenkova et al., 2018).

The Vendian Vilchitsy Group is divided into the Blonsk and Glusk formations. The Blonsk Formation (thickness 245 m) is mainly represented by the fine-grained feldspar- and quartz-rich sandstones with subordinate fragments of granitoids, sandstones, and sandy-dolomitic rocks. Layers of claystones and boulder-pebble conglomerates are also found in the sections (*Geologiya* ..., 2001). The Glusk Formation (483 m) is composed of tillites, oligomictic sandstones, siltstones, and silty–clayey rocks. The latter rocks are sometimes characterized by the varved bedding with megaclasts (pebbles, gravel, and sand–gravel accumulations).

The Volyn Group includes the Gorbasi, Rataichitsy, Kletsk, Lukoml, Girsk, Vidibor, and Liozno formations. The Gorbashi Formation (30 m) is composed of the coarse- and varigrained arkosic sandstones with siltstones interlayers. The Rataichitsy Formation (340 m) is composed of basalts, dolerite basalts, their lava breccias and tuffs, andesidacites, dacites, and trachyrhyodacites (*Geologiya* ..., 2001; Makhnach et al., 1976; and others). The Kletsk Formation (177 m) is represented by tuffs (psammitic, silty, and clayey-silty), tuffites, tuffaceous sandstones, and tuffaceous siltstones. The Lukoml Formation (80 m) unites the tuffogenic and tuffogenic-sedimentary rocks (tuffites, tuffogenic and/or volcanomictic-arkosic sandstones and siltstones), as well as gravelites. The Rataichitsy, Kletsk, and Lukoml formations are considered as different-facies stratigraphic analogs (*Stratigraficheskie* ..., 2010). The Girsk Formation (110 m) is composed of the red-colored, coarse- and varigrained arkosic and volcanomictic sandstones, gravelites, gravel-pebble conglomerates, and sandy and clayey siltstones. The Vidibor Formation (up to 70 m) unites the volcanomictic and polymictic sandstones, clayey siltstones, and clays (*Geologiya* ..., 2001; Makhnach et al., 1976). The Liozno Formation (50 m) is represented by the heterogeneous volcanomictic and arkosic (mainly coarse-grained) sandstones with siltstone interlayers. The rocks contain glauconite. The Liozno, Girsk, and Vidibor formations are considered stratigraphic analogs (*Stratigraficheskie* ..., 2010).

The Valdai Group unites the Nizov, Selyavy, Tshernitsa, and Kotlin formations. The first three formations belong to the Vendian Redkino regional stage; the Kotlin Formation, to the eponymous regional stage. The Nizov Formation (47 m) is mainly represented by the coarse- and medium-grained volcanomictic sandstones and siltstones (*Geologiya* ..., 2001; Laptsevich et al., 2023; *Stratigraficheskie* ..., 2010). The Selyavy Formation (57 m) is composed of the micaceous siltstones and silty mudstones, with interlayers of the fine-grained micaceous arkosic sandstones in the lower part (Golubkova et al., 2022). The Tshernitsa Formation (64 m) is represented mainly by clays and micaceous siltstones, with siltstones and heterogeneous arkosic sandstones in the lower part. Pyrite is quite typical for rocks of this stratigraphic level (Golubkova et al., 2022). The Kotlin Formation (up to 220 m) includes various combinations of the heterogeneous arkosic (quartz and feldspar–quartz in the upper part) sandstones, mudstones and silty varieties, micaceous siltstones, siderites, and mudstones with glauconite.

According to the data in (Jewuła et al., 2022), the fine-grained clastic rocks of the Volyn level in western Belarus (boreholes Kormyanskaya and Bykhovskaya) and Volhynia are characterized by an average quartz content of ~14.0 ± 8.0 wt %, increasing upsection in Kotlin mudstones to ~30.0 wt % (hereinafter, results of the determination of the quantitative mineral composition of claystones using the XRD analysis of bulk samples are given). The content of potassium feldspar (Kfs) is approximately constant (wt %): 11.0 ± 7.0 (Volyn stratigraphic level), 17.0 ± 7.0 (Redkino level), and 14.0 ± 9.0 (Kotlin level). The average plagioclase content decreases from ~6.0 (Volyn level) to 0.2 wt % (Kotlin level). The average content of $1M_d$ illite in the fine-grained clastic rocks is as follows (wt %): 15.0 ± 9.0 (Volyn stratigraphic level), 19.0 ± 10.0 (Redkino level), and 13.0 ± 9.0 (Kotlin). The average content of different varieties of smectite is maximum (20.0 ± 18.0 wt %) in claystones of the Volyn level and 6.0 ± 7.0 wt % in the rocks of the Kotlin regional stage with the same grain size composition. The content of kaolinite does not change significantly upward the section. The average content is as follows: 10.0 wt % in rocks of the Volyn level, about 18.0 wt % in the Redkino regional stage, and ~15.0 wt % in the Kotlin regional stage. It should be emphasized that the kaolinite, illite, and smectites can be absent or dominant in different samples: up to 35.0–40.0 wt % (illite and kaolinite) and less often 65.0 wt % (smectites). The average chlorite content can vary from 1.0 ± 2.0 (Kotlin level) to 3.0 ± 3.7 wt % (Volyn level). Its maximum content in the sample does not exceed 10.0 wt %. The fine-grained rocks under consideration are also marked by the presence of authigenic berthierine (Redkino and Kotlin regional stages), which is associated with the transformation of kaolinite. The average berthierine content varies from 3.0 ± 4.0 to 4.0 ± 6 wt % and can reach 25.0 wt % in some samples. The total content of clay components in the fine-grained clastic rocks of

this region varies from 37.0 (Kotlin level) to 44.0 wt % (Redkino level).

In eastern Belarus (boreholes Lepel 1 and Bogushevskaya 1), the situation is somewhat different. The content of $1M_d$ illite in the fine-grained clastic rocks and the Volyn–Kotlin interval averages 12.0–13.0 wt %. The content of various smectites varies from slightly more than 13.0 wt % (Volyn level) to 9.0 wt % (Redkino), and 11.0 wt % (Kotlin). Taking into account the probable errors, these values are statistically comparable. On the contrary, the average kaolinite content in claystones of the Volyn level is only 10.0 ± 7.0 wt %. The content is as high as 18.0 ± 5.0 wt % in rocks of the Redkino regional stage and 17.0 ± 7.0 wt % in the Kotlin rocks (Jewuła et al., 2022). The highest average content of clay components is typical for the fine-grained clastic rocks of the Redkino and Kotlin levels: 46.0 ± 15.0 and 45.0 ± 16.0 wt %, respectively. In rocks of the Volyn Group, their content is slightly lower: 39.0 ± 16.0 wt %. At the same time, the distribution of illite, kaolinite, chlorite, and smectite in different samples is similar to that in claystones of western Belarus and Volhynia. In the Vendian claystones of this region, berthierine occurs at all of the studied stratigraphic levels: its average content is slightly higher than in similar rocks from the western part of Belarus and Volhynia (5.0–6.4 ± 5.0–7.0 wt %). The maximum contents are also slightly higher (up to 28.0 wt % in mudstones of the Kotlin level). In addition to these minerals, goethite, hematite, pyrite, sulfates, siderite, apatite, and carbonate minerals are found in the fine-grained clastic rocks of the Volyn and Valdai groups in Belarus and Volhynia.

DEPOSITIONAL SETTING OF THE RIPHEAN AND VENDIAN SEDIMENTARY SEQUENCES

According to (Kuzmenkova et al., 2018, 2019a, 2019b, and references therein), the Rogachev and Rudnya formations are represented, by shallow epicontinental sediments of a freshened (to a variable extent) basin. The Orsha Formation reflects the depositional stage in a shallow closed (intracontinental) basin with low salinity. The data in (Golubkova et al., 2022; Jewuła et al., 2022; *Paleogeografiya* ..., 1980) suggest that the Vendian rocks were deposited here mainly in alluvial fans, channel and floodplain zones, as well as coastal (lagoonal included) and shallow-sea environments (Kuzmenkova et al., 2018; Laptsevich et al., 2023). In most cases, deposits of these environments can inherit the "provenance signal"—the distribution of several low soluble trace elements (Th, La, Sc, Co, Cr, V, and others), as well as their relationships in the provenance (*Geochemistry* ..., 2003; *Interpretatsiya* ..., 2001; McLennan, 1989; McLennan et al., 1990, 1993; Taylor and McLennan, 1985; and others). This feature is most characteristic of the fine-grained clastic rocks containing a significant proportion of the clay component.

FACTUAL MATERIAL

To study the lithogeochemistry of sandstones and siltstones from the Riphean (Rogachev, Rudnya, and Orsha formations) and Vendian (Glusk, Lukoml, Liozno, Nizov, Selyavy, Tshernitsa, and Kotlin formations) sectons, we used a collection of 54 samples taken from boreholes Bogushevskaya 1, Bykhovskaya, Lepel 1, and Kormyanskaya during the joint work of the Institute of Precambrian Geology and Geochronology (St. Petersburg) and the National Production Center for Geology (Minsk). Borehole Bogushevskaya 1 is located in the southern Vitebsk region (30–40 km south of Vitebsk near the eponymous settlement. Borehole Bykhovskaya was drilled at the Gomel/Mogilev border about 100 km north of Gomel. Borehole Lepel 1 is located in the western Vitebsk region (90–100 km west of Vitebsk). Borehole Kormyanskaya is located in the northern Gomel region (70–80 km north of Gomel near the Korma Settlement). A detailed lithological and paleontological description of the Vendian rocks is presented in (Golubkova et al., 2021; Kuzmenkova et al., 2018; Laptsevich et al., 2023; Streltsova et al., 2023). The sample collection covers all stratigraphic levels and main lithotypes in the Riphean and Vendian rocks recovered by these boreholes. Taking into account several individual lithostratigraphic units (formations), the total number of samples in our collection is not yet statistically representative. Nevertheless, we believe that the following conclusions based on the results of the pilot project are quite correct.

The content of the major oxides in sandstones and siltstones was determined by the X-ray fluorescence method using an ARL 9800 (VSEGEI, St. Petersburg) X-ray spectrometer. The lower detection limit was as follows (wt %): 0.02 (SiO_2), 0.01 (TiO_2), 0.05 (Al_2O_3), 0.01 ($Fe_2O_3^* = FeO + Fe_2O_3$), 0.01 (MnO), 0.1 (MgO), 0.01 (CaO), 0.1 (Na_2O), and 0.01 (K_2O).

The content of trace elements was determined using a quadrupole mass spectrometer equipped with ICP Agilent 7700x (VSEGEI, St. Petersburg). The lower limits for the determination of element concentrations were as follows (μg/g): 3 (Ba), 2.5 (V), 2 (Rb), 1 (Cr, Ni, Sr, Pb, and Zn), 0.5 (Co, Zr, Nb), 0.2 (Sc), 0.1 (Ga, Y, Cs, Th, U), 0.01 (La, Ce, Pr, Nd, Gd, Dy, Er, Yb, Hf), and 0.005 (Sm, Eu, Tb, Ho, Tm, Lu). Their distribution relative to various reference geochemical objects is discussed below.

The bulk chemical composition of the studied sandstone and siltstone samples is presented in Tables 1 and 2. Hereinafter, the content of all major oxides is given in wt %.

Under the program of pilot studies, we studied the chemical composition of sandstones and siltstones both to elucidate the lithotype visually identified during the sampling and to obtain additional information about the mechanisms and processes of their for-

Table 1. Content of the major oxides (wt %) and values of the lithochemical modules for the representative samples of Upper Precambrian sandstones (SN) and siltstones (SL) in Belarus

Components	Borehole															
	Kormyanskaya			Bykhovskaya			Bogushevskaya 1									
	Formation															
	Rogachev			Rudnya			Orsha				Glusk				Lukoml	
	Rocks															
	SN	SN	SN	SL	SN	SL	SN	SL	SL	SN	SL	SN	SL	SN	SL	SL
	Prefix															
	Km-			Bh-			Bo-			Bh-					Bo-	
	Sample no.															
	648	662	350	716	735	758	893	1489	1547	706	383	460	611	691	760	772
SiO_2	96.90	98.50	92.60	79.50	81.10	84.00	98.30	93.90	87.80	82.40	60.90	88.70	63.30	96.80	55.30	56.70
TiO_2	0.01	0.01	0.28	0.04	0.09	0.01	0.01	0.19	0.38	0.11	0.96	0.26	0.86	0.01	1.59	1.71
Al_2O_3	1.13	0.33	2.50	10.70	11.00	8.35	0.13	2.50	4.00	9.98	14.50	5.09	13.70	1.16	15.20	16.70
$Fe_2O_3^*$	0.38	0.26	0.83	0.76	0.59	0.33	0.29	0.98	2.39	0.73	8.90	0.79	9.29	0.20	11.50	10.00
MnO	0.01	0.01	0.01	0.01	0.01	0.01	0.01	0.01	0.01	0.01	0.98	0.01	0.05	0.01	0.10	0.03
MgO	0.10	0.10	0.10	0.10	0.43	0.10	0.10	0.10	0.35	0.10	2.15	0.39	1.74	0.10	3.46	2.54
CaO	0.19	0.17	0.16	0.12	0.14	0.15	0.18	0.11	0.28	0.10	0.47	0.26	0.40	0.13	1.25	0.64
Na_2O	0.09	0.09	0.09	0.08	0.10	0.10	0.10	0.09	0.09	0.09	0.26	0.09	0.20	0.10	1.03	1.00
K_2O	0.64	0.42	2.30	5.39	4.07	5.31	0.01	0.06	2.45	4.29	5.71	2.59	5.82	0.82	4.33	5.06
P_2O_5	<0.05	<0.05	<0.05	<0.05	<0.05	<0.05	<0.05	<0.05	<0.05	<0.05	0.15	<0.05	0.14	<0.05	0.32	0.11
LOI	0.35	0.36	0.70	2.72	2.33	1.67	0.38	1.47	1.39	2.65	4.75	1.78	3.96	0.59	5.42	5.26
Total	99.70	100.00	99.40	99.20	99.80	99.80	99.30	99.20	99.10	100.00	99.80	100.00	99.50	99.70	99.50	99.80
$Na_2O + K_2O$	0.73	0.51	2.39	5.47	4.17	5.41	0.11	0.15	2.54	4.38	5.97	2.68	6.02	0.92	5.36	6.06
HM	0.016	0.006	0.039	0.14	0.14	0.10	0.004	0.04	0.08	0.131	0.42	0.07	0.38	0.014	0.51	0.50
FM	0.005	0.004	0.01	0.011	0.013	0.005	0.004	0.012	0.031	0.010	0.20	0.013	0.18	0.003	0.27	0.22
TM	0.008	0.028	0.112	0.004	0.008	0.001	0.067	0.076	0.095	0.011	0.066	0.051	0.063	0.008	0.11	0.10
IM	0.34	0.80	0.30	0.07	0.05	0.04	2.16	0.37	0.55	0.07	0.64	0.15	0.64	0.18	0.69	0.54
NAM	0.65	1.54	0.96	0.51	0.38	0.65	0.81	0.06	0.64	0.44	0.41	0.53	0.44	0.79	0.35	0.36
AM	0.14	0.21	0.04	0.02	0.02	0.02	9.50	1.41	0.04	0.02	0.05	0.03	0.03	0.12	0.24	0.20

Table 1. (Contd.)

Components	Borehole															
	Lepel 1		Bogushevskaya 1					Lepel 1	Bogushevskaya 1						Lepel 1	
	Formation															
	Liozno			Nizov		Selyavy			Tshernitsa			Kotlin				
	Rocks															
	SL	SL	SL	SN	SL	SL	SL	SN	SL	SL	SN	SL	SL	SL	SL	SN
	Prefix															
	Lp-		Bo-					Lp-	Bo-						Lp-	
	Sample no.															
	528	540	721	681	685	658	660	477	600	608	622	515	521	530.5	329	378
SiO_2	61.10	52.20	49.20	76.70	60.90	58.60	57.00	82.40	61.20	56.20	65.10	58.40	61.00	68.50	56.00	81.70
TiO_2	1.85	1.30	1.60	0.37	0.90	1.45	1.48	0.29	0.96	1.29	0.06	1.24	1.01	1.03	1.06	0.21
Al_2O_3	16.70	18.90	22.30	4.88	8.14	18.20	19.50	9.06	15.90	18.60	7.06	19.10	15.60	15.20	23.60	4.15
$Fe_2O_3^*$	7.88	10.30	10.50	1.86	2.80	6.84	7.78	0.62	6.89	7.27	3.05	6.36	6.07	3.59	5.96	1.01
MnO	0.05	0.06	0.06	0.38	0.69	0.03	0.03	0.01	0.31	0.21	0.50	0.18	0.22	0.03	0.02	0.03
MgO	1.47	4.41	2.04	2.00	3.82	1.72	1.84	0.13	1.48	2.34	2.98	1.47	1.23	0.92	1.64	0.12
CaO	0.64	0.66	0.40	4.51	7.23	0.46	0.34	0.27	0.82	1.30	6.86	0.30	2.17	0.28	0.21	6.22
Na_2O	1.23	1.19	0.73	0.22	0.39	1.05	0.95	0.53	0.50	0.48	0.22	0.75	0.33	0.63	0.09	0.09
K_2O	4.43	4.34	4.14	2.02	2.82	4.14	4.26	4.84	4.71	4.42	3.39	3.98	4.22	3.92	3.51	2.21
P_2O_5	<0.05	0.13	0.13	<0.05	<0.05	<0.05	0.06	<0.05	0.06	0.82	<0.05	<0.05	<0.05	0.07	0.08	0.08
LOI	4.70	6.61	8.57	6.71	12.00	7.27	6.62	1.83	6.75	7.02	10.50	7.56	8.08	5.02	8.28	3.91
Total	100.00	100.00	99.70	99.70	99.70	99.80	99.90	100.00	99.50	100.00	99.70	99.40	99.90	99.30	100.00	99.60
$Na_2O + K_2O$	5.66	5.53	4.87	2.24	3.21	5.19	5.21	5.37	5.21	4.90	3.61	4.73	4.55	4.55	3.60	2.30
HM	0.43	0.59	0.70	0.10	0.21	0.45	0.51	0.121	0.39	0.49	0.164	0.46	0.38	0.28	0.29	0.066
FM	0.15	0.28	0.26	0.06	0.12	0.15	0.17	0.009	0.14	0.18	0.10	0.14	0.12	0.066	0.066	0.014
TM	0.111	0.069	0.072	0.076	0.111	0.080	0.076	0.032	0.060	0.069	0.009	0.065	0.065	0.070	0.068	0.051
IM	0.43	0.51	0.44	0.43	0.39	0.35	0.37	0.07	0.43	0.38	0.50	0.32	0.38	0.23	0.22	0.24
NAM	0.34	0.29	0.22	0.46	0.39	0.29	0.27	0.59	0.33	0.26	0.51	0.25	0.29	0.30	0.30	0.56
AM	0.28	0.27	0.18	0.11	0.14	0.25	0.22	0.11	0.11	0.11	0.06	0.19	0.08	0.26	0.16	0.04

Table 2. Content of trace elements (μg/g) in the representative samples of Upper Precambrian sandstones (SN) and siltstones (SL) in Belarus

Components	Borehole															
	Kormyanskaya			Bykhovskaya			Bogushevskaya 1									
	Formation															
	Rogachev		Rudnya				Orsha			Glusk					Lukoml	
	Rocks															
	SN	SN	SN	SL	SN	SL	SN	SL	SL	SN	SL	SN	SL	SN	SL	SL
	Prefix															
	Km-			Bh-			Bo-			Bh-					Bo-	
	Sample no.															
	648	662	350	716	735	758	893	1489	1547	706	383	460	611	691	760	772
Sc	1.34	1.08	3.49	1.66	2.09	1.38	1.24	4.48	7.21	2.55	11.70	3.61	10.70	1.34	18.80	20.20
V	<2.50	2.81	17.80	3.21	5.36	<2.50	5.01	3.33	10.10	11.20	49.50	18.20	46.10	<2.50	172.00	197.00
Cr	6.91	10.70	12.50	8.61	7.55	5.66	4.87	8.04	11.00	6.99	46.10	13.60	41.20	6.51	53.50	60.10
Co	333.00	312.00	258.00	66.00	177.00	122.00	218.00	103.00	145.00	122.00	27.60	280.00	32.10	305.00	41.00	26.20
Ni	4.72	6.78	5.52	2.88	2.96	2.87	3.01	4.52	12.50	4.15	32.40	11.40	26.40	4.76	35.80	29.40
Zn	1.47	<1.00	16.20	<1.00	<1.00	<1.00	<1.00	<1.00	24.40	2.71	110.00	30.30	79.80	<1.00	76.70	76.40
Ga	1.16	1.03	3.77	8.31	6.52	6.39	0.77	2.95	6.57	7.78	20.70	6.73	18.00	1.85	20.10	20.50
Rb	14.60	9.79	49.10	113.00	79.40	113.00	<2.00	2.17	71.30	102.00	164.00	71.20	151.00	17.70	117.00	144.00
Sr	12.60	16.70	75.80	67.40	53.50	63.80	12.90	27.20	75.10	64.70	107.00	46.30	138.00	39.90	84.70	88.30
Y	4.24	3.45	11.80	4.79	5.86	3.56	3.94	14.00	34.50	7.81	27.80	10.30	26.20	4.20	35.00	32.80
Zr	28.40	21.40	219.00	37.00	59.20	29.20	32.20	253.00	287.00	98.20	230.00	107.00	268.00	19.90	187.00	159.00
Nb	0.57	<0.50	5.20	2.08	3.13	1.19	0.54	3.89	6.46	3.91	36.00	7.02	37.30	0.69	20.60	19.20
Cs	0.28	0.26	0.58	1.03	0.79	0.97	<1.00	<1.00	2.20	1.04	5.94	1.46	5.43	0.24	3.20	3.68
Ba	93.40	58.00	930.00	909.00	629.00	930.00	28.20	16.80	322.00	788.00	519.00	389.00	576.00	279.00	458.00	459.00
La	6.36	9.13	18.10	10.50	9.87	7.10	5.00	11.20	15.60	12.60	47.70	16.00	69.10	9.04	51.40	47.80
Ce	8.13	8.71	34.60	18.20	25.10	15.40	8.49	22.30	32.90	23.80	111.00	33.40	128.00	16.20	103.00	98.20
Pr	1.33	1.85	4.08	2.62	2.36	1.51	1.32	2.92	3.81	3.10	10.70	3.95	13.40	2.23	12.70	11.80
Nd	4.87	6.40	15.00	9.67	8.68	5.58	5.14	11.30	14.70	11.80	36.00	14.10	39.70	8.28	49.60	44.90
Sm	0.90	1.04	2.63	1.52	1.62	0.90	0.94	2.42	3.47	2.01	6.30	2.61	5.57	1.38	9.65	8.50
Eu	0.19	0.17	0.56	0.49	0.47	0.39	0.18	0.50	0.92	0.58	1.33	0.54	1.12	0.31	2.03	1.96
Gd	0.73	0.72	2.22	1.06	1.28	0.77	0.79	2.34	4.37	1.58	6.19	2.13	5.53	1.08	8.51	7.51
Tb	0.12	0.11	0.32	0.15	0.19	0.11	0.12	0.38	0.83	0.23	0.94	0.31	0.83	0.15	1.22	1.11
Dy	0.75	0.58	1.91	0.81	1.04	0.63	0.66	2.25	5.50	1.35	5.17	1.77	4.74	0.77	6.95	6.51
Ho	0.15	0.12	0.39	0.17	0.21	0.12	0.13	0.45	1.18	0.28	1.02	0.37	0.95	0.15	1.33	1.25
Er	0.45	0.36	1.17	0.50	0.62	0.37	0.36	1.34	3.50	0.81	2.87	1.04	2.75	0.42	3.70	3.64
Tm	0.07	0.06	0.19	0.08	0.09	0.06	0.05	0.20	0.54	0.12	0.44	0.16	0.41	0.06	0.50	0.53
Yb	0.45	0.38	1.21	0.51	0.63	0.38	0.37	1.37	3.62	0.84	2.84	1.06	2.86	0.41	3.28	3.45
Lu	0.07	0.06	0.20	0.08	0.10	0.06	0.06	0.21	0.56	0.12	0.42	0.16	0.43	0.06	0.49	0.50
Hf	0.89	0.69	6.26	1.16	1.89	0.94	0.94	7.37	8.01	2.93	6.73	3.12	7.56	0.65	5.69	4.76
Pb	1.30	1.19	5.48	3.16	2.19	2.75	1.90	2.23	3.89	3.22	12.90	3.09	10.20	1.41	7.55	5.80
Th	0.99	0.92	6.04	1.79	2.15	1.32	0.76	3.12	7.45	2.84	13.90	3.60	12.60	1.17	10.00	8.72
U	0.30	1.24	0.84	0.42	0.55	0.29	0.31	1.11	2.78	0.65	2.47	4.53	2.26	0.36	1.56	2.10

Table 2. (Contd.)

Components	Borehole															
	Lepel 1		Bogushevskaya 1					Lepel 1	Bogushevskaya 1						Lepel 1	
	Components															
	Liozno			Nizov		Selyavy			Tshernitsa			Kotlin				
	Rocks															
	SL	SL	SL	SN	SL	SL	SL	SN	SL	SL	SN	SL	SL	SL	SL	SN
	Prefix															
	Lp-		Bo-					Lp-	Bo-						Lp-	
	Sample no.															
	528	540	721	681	685	658	660	477	600	608	622	515	521	530.5	329	378
Sc	18.70	18.40	19.20	4.92	15.60	14.30	14.50	3.11	10.80	17.60	3.72	14.40	10.40	11.20	14.60	2.40
V	72.00	82.00	182.00	11.20	29.70	93.40	102.00	13.90	69.60	101.00	12.60	85.50	52.80	66.20	102.00	13.20
Cr	41.50	84.80	87.40	14.50	28.30	60.20	65.30	18.10	46.30	64.70	9.31	65.30	42.60	47.30	72.30	14.60
Co	29.60	55.10	23.50	66.70	46.50	25.80	23.20	179.00	38.50	37.60	50.90	51.50	29.40	28.30	30.40	72.30
Ni	23.10	59.20	35.30	6.95	8.02	23.40	24.70	3.15	21.70	26.70	3.49	34.50	17.40	25.60	41.50	4.65
Zn	52.30	116.00	86.50	3.16	7.52	148.00	62.70	1.22	40.00	76.20	<1.0	213.00	65.60	72.50	86.80	1.74
Ga	20.00	24.80	27.80	5.00	10.10	21.40	24.50	6.17	18.70	26.20	6.24	21.40	17.00	18.40	25.00	5.03
Rb	124.00	142.00	150.00	45.10	65.20	138.00	144.00	106.00	144.00	201.00	92.00	156.00	155.00	121.00	175.00	52.70
Sr	164.00	130.00	138.00	117.00	77.30	144.00	155.00	109.00	104.00	309.00	153.00	85.40	105.00	304.00	239.00	739.00
Y	39.70	52.10	37.60	22.20	38.20	28.90	24.70	8.04	29.20	69.80	15.80	34.40	32.00	30.30	28.10	6.57
Zr	615.00	355.00	207.00	221.00	756.00	290.00	243.00	145.00	287.00	321.00	61.50	213.00	274.00	319.00	113.00	60.90
Nb	24.80	18.10	25.20	5.51	13.30	21.40	22.40	4.51	15.10	21.60	1.56	21.50	17.40	16.30	17.70	3.25
Cs	2.35	3.25	4.83	0.24	0.47	3.04	3.43	0.59	2.40	4.29	0.46	4.22	2.85	3.09	4.38	0.35
Ba	767.0	602.0	572.0	1850.0	654.0	839.0	831.0	1000.0	869.0	896.0	992.0	626.0	1020.0	672.0	615.0	408.0
La	67.50	77.80	89.00	25.40	56.80	65.50	69.20	22.10	53.70	93.20	20.20	54.80	47.60	71.00	63.30	12.30
Ce	142.00	154.00	175.00	57.40	120.00	128.00	138.00	46.70	109.00	197.00	42.20	107.00	95.50	159.00	124.00	23.30
Pr	15.60	19.50	20.90	7.23	14.70	15.00	16.40	4.77	12.80	23.90	4.86	12.80	11.00	18.50	12.90	2.98
Nd	56.90	75.50	76.50	29.60	57.60	54.50	59.60	16.60	47.90	91.80	20.50	47.00	41.00	67.40	44.50	11.10
Sm	10.20	14.40	13.30	6.06	11.50	8.77	9.61	2.68	8.52	16.80	4.55	8.43	7.46	10.10	7.19	2.13
Eu	1.78	2.37	2.44	1.54	1.80	1.68	1.92	0.99	1.76	3.96	1.54	1.61	1.48	1.72	1.50	0.62
Gd	8.73	12.00	10.70	5.43	9.59	7.25	7.37	2.07	7.22	16.70	3.88	7.10	6.31	6.51	6.50	1.73
Tb	1.28	1.68	1.54	0.82	1.33	1.04	1.00	0.28	1.02	2.45	0.56	1.08	0.96	0.87	0.98	0.25
Dy	7.68	9.24	8.22	4.49	6.92	5.82	5.32	1.61	5.48	13.20	3.12	6.06	5.59	5.05	5.69	1.35
Ho	1.56	1.81	1.55	0.78	1.26	1.11	1.01	0.31	1.05	2.40	0.58	1.22	1.09	1.07	1.12	0.25
Er	4.50	4.95	4.33	1.92	3.50	3.18	2.91	0.92	2.97	5.96	1.46	3.62	3.28	3.34	3.06	0.68
Tm	0.67	0.68	0.62	0.24	0.50	0.47	0.42	0.14	0.41	0.73	0.19	0.53	0.49	0.53	0.43	0.10
Yb	4.53	4.23	4.05	1.48	3.45	3.13	2.75	0.95	2.74	4.16	1.07	3.51	3.01	3.68	2.68	0.67
Lu	0.69	0.65	0.60	0.23	0.56	0.45	0.42	0.16	0.41	0.62	0.15	0.52	0.46	0.56	0.41	0.10
Hf	17.80	10.20	6.50	6.24	22.30	8.76	7.44	4.13	8.50	8.90	1.82	6.66	8.27	9.69	3.65	1.89
Pb	8.06	6.96	10.30	4.55	6.51	8.55	8.29	9.44	8.37	5.95	5.93	7.57	5.91	4.45	5.34	1.76
Th	28.60	24.50	21.80	7.93	26.00	18.00	17.10	4.34	19.40	20.60	2.41	14.90	15.90	12.40	10.60	3.65
U	2.88	2.35	2.35	0.89	3.19	1.76	1.62	0.61	2.32	2.99	0.22	4.36	2.52	2.98	2.97	0.60

mation (provenance and paleoclimate included). For this purpose, we used the chemical classification of rocks proposed by Y.E. Yudovich and M.P. Ketris (2000), as well as several other diagrams that contribute to solve these problems. The chemical certification of rocks was carried out using various ratios (modules) based the content of major oxides (in wt%): hydrolyzate module, HM = $(Al_2O_3 + TiO_2 + Fe_2O_3^* + MnO)/SiO_2$, femic module, FM = $(Fe_2O_3^* + MnO + MgO)/SiO_2$, titanium module, TM = TiO_2/Al_2O_3, iron module, IM = $(Fe_2O_3^* + MnO)/(Al_2O_3 + TiO_2)$, normalized alkalinity (NM + KM) module, NAM = $(Na_2O + K_2O)/Al_2O_3$, and alkalinity module, AM = Na_2O/K_2O.

CHEMICAL CLASSIFICATION OF ROCKS AND SOME PECULIARITIES IN THE DISTRIBUTION OF MAJOR OXIDES

Sandstones

The first peculiarity in the chemical classification of sandstones is their rather distinct discrimination into three clusters in the main, according to (Yudovich and Ketris, 2000), $(Na_2O + K_2O)$–HM and $(Na_2O + K_2O)/Al_2O_3$–$(Al_2O_3 + TiO_2 + Fe_2O_3^* + MnO)/SiO_2$ diagrams (Figs. 2a, 2b). Cluster 1 includes Late Riphean sandy rocks of the Rogachev (sample Km-648, 662) and Orsha (Bo-893, 1518) formations along with the Lower Vendian Glusk Formation (Bh-634, 691) with the highest SiO_2 (96.8–98.5%) and the least alkali contents ($Na_2O + K_2O < 0.92\%$). They belong to hypersilites with HM < 0.016 and NAM = 0.10–1.54 (average 0.79). Samples of this cluster are characterized by the minimum (in the sample set) content of TiO_2 (usually <0.01%), except sample Bo-1518 (~0.04%), as well as lower concentrations of $Fe_2O_3^*$ (0.2–0.4%). Nevertheless, these rocks are generally characterized by higher values of FM and lower values of TM, relative to rocks in cluster 2 (Fig. 2c). Together with high TM values and low TiO_2 content, such low HM values are most typical for the quartz-rich varieties of sandstones (Yudovich and Ketris, 2000). This statement is also consistent with the distribution of data points of sandy rocks in cluster 1 in $\log(SiO_2/Al_2O_3)$–$\log(Na_2O/K_2O)$ (Pettijohn et al., 1976) and $\log(SiO_2/Al_2O_3)$–$\log(Fe_2O_3^*/K_2O)$ (Herron, 1988) diagrams: in both diagrams, they fall into the field of quartz arenites (Figs. 3a, 3b).

Cluster 2 includes the hyper- and supersilites of the Rudnya Formation (samples Km-350, Km-438, Km-518), the Glusk Formation, as well as single samples of the Nizov (Bo-681) and Kotlin formations (Lp-378) characterized by HM = 0.036–0.098 and NAM = 0.46–1.01. The SiO_2 content in these rocks is 88.7–93.6% and rarely less (76.7–81.7%). The latter value is probably related to the development of carbonate cement and the corrosion of quartz grains in the Nizov and Kotlin formations (CaO 4.5–6.2%, LOI 3.9–6.7%), since the total alkali content in these samples is almost the same as in other sandstones of this cluster. It should be emphasized that, in general, the total alkali content in sandstones of cluster 2 are notably higher (1.9–3.4%) than in rocks of cluster 1. Rocks of cluster 2 are enriched in Ti and depleted in IM, relative to sandstones of cluster 1 (Table 1, Fig. 2c). Based on HM values and the distribution of data points in cluster 2 of $\log(SiO_2/Al_2O_3)$–$\log(Na_2O/K_2O)$ and $\log(SiO_2/Al_2O_3)$–$\log(Fe_2O_3^*/K_2O)$ diagrams (Figs. 3a, 3b), these rocks belong to both quartz-rich and oligomictic (most likely, feldspar–quartz) varieties of sandstones.

Cluster 3 includes samples taken from the Rudnya (Bh-735), Orsha (Bh-706), Selyavy (Lp-477), and Tshernitsa (Bo-622) formations. They are distinguished by the minimum (among the studied sandstones) content of SiO_2 (65.1–81.1...82.4%) and the higher $(Na_2O + K_2O)$ values (Fig. 2b, Table 1). Sandstones of cluster 3 are marked by the minimum TM and IM values (Fig. 2c), while NAM and HM values are maximum (Fig. 2b). In accordance with the lithochemical classification (Yudovich and Ketris, 2000), sandstones of this cluster are normosilites. They can include the arkosic, feldspar–quartz sandstones, and felsic graywackes. In our case, judging from the position of data points in the $\log(SiO_2/Al_2O_3)$–$\log(Na_2O/K_2O)$ and $\log(SiO_2/Al_2O_3)$–$\log(Fe_2O_3^*/K_2O)$ diagrams, they are probably arkoses (Figs. 3a, 3b). Sample Bo-622 in this cluster likely contains dolomite and/or calcite in the cement (MgO ~3.0%, CaO ~6.9%, LOI 10.5%).

Thus, sandy rocks in the pilot collection are quite consistent (in chemical composition) with sandstones, and the distribution of major oxides in them and the geochemical certification (based on modules) allow us to classify them as quartz-rich and oligomictic (probably, feldspar–quartz) varieties, as well as arkoses. Some samples containing the carbonate cement should be used with caution in further lithogeochemical studies.

Comparison of the lithochemical parameters of Riphean and Vendian sandstones in the available material with the average UCC composition (Rudnick and Gao, 2003) did not identify any definite patterns of their temporal composition evolution (Fig. 4). It is obvious that the established geochemical differences or similarities of sandstones are related to their affiliation to one of the three lithotypes. At the same time, we can note the similarity of the bulk chemical composition of some sandstone samples from the Riphean Rudnya and Orsha formations with individual sand-

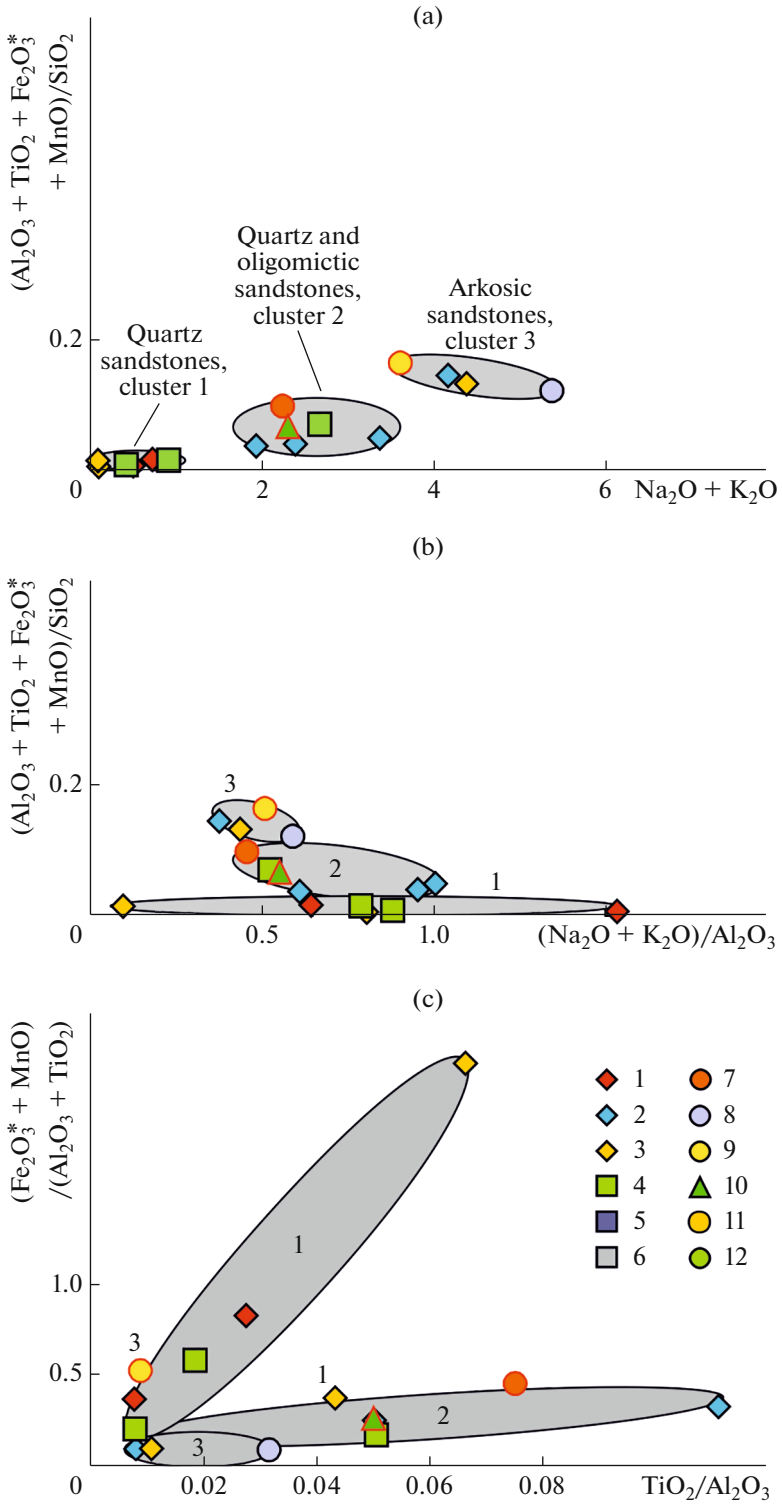

Fig. 2. Position of data points of sandstones from different formations in module diagrams $(Na_2O + K_2O)$–$(Al_2O_3 + TiO_2 + Fe_2O_3^* + MnO)/SiO_2$ (a) and $(Na_2O + K_2O)/Al_2O_3$–$(Al_2O_3 + TiO_2 + Fe_2O_3^* + MnO)/SiO_2$ (b), and TiO_2/Al_2O_3–$(Fe_2O_3^* + MnO)/(Al_2O_3 + TiO_2)$ (c). (1–10) Formations: (1) Rogachev, (2) Rudnya, (3) Orsha, (4) Glusk, (5) Lukoml, (6) Liozno, (7) Nizov, (8) Selyavy, (9) Tshernitsa, (10) Kotlin; (11) all studied sandstones; (12) all studied siltstones and claystones. Legend with red contours shows the carbonatized rock varieties.

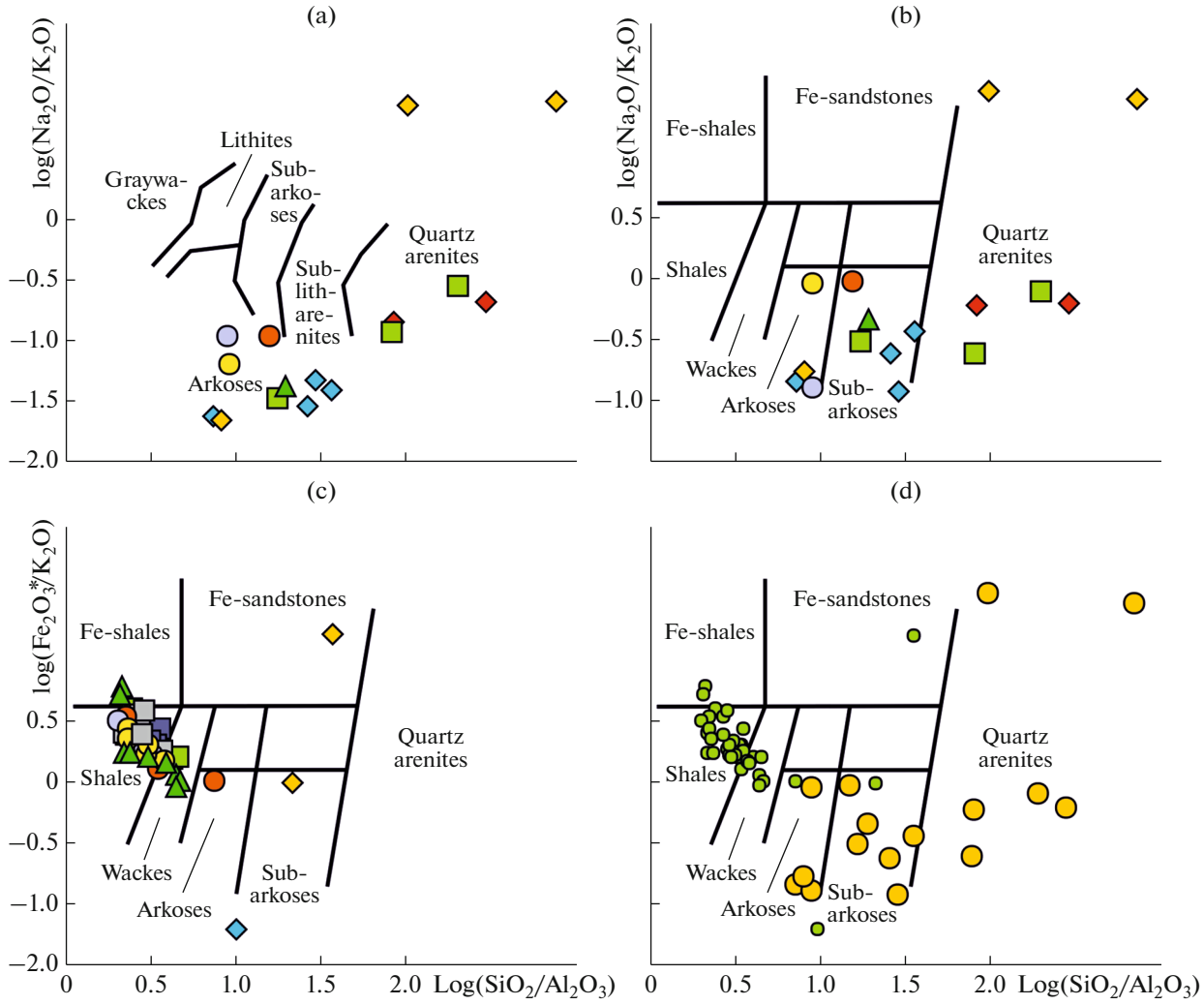

Fig. 3. Position of data points of sandstones (a, b), siltstones and mudstones from various formations (c), as well as their sample sets (d) on classification diagrams $\log(SiO_2/Al_2O_3)$–$\log(Na_2O/K_2O)$ (Pettijohn et al., 1976) (a) and $\log(SiO_2/Al_2O_3)$–$\log(Fe_2O_3^*/K_2O)$ (Herron, 1988) (b–d). Legend as in Fig. 2.

stone samples from the Lower Vendian Glusk formation, as well as Nizov and Tshernitsa sandstones.

All the listed lithotypes (or petrotypes) of sandstones, identified by interpreting their chemical compositional features, do not contradict the data based on the general lithological characteristics of formations and the material presented above in section "Lithostratigraphy and Composition ...", which indicates correctness of the performed geochemical studies and provides perspectives for their further application.

Siltstones

The geochemical attestation of siltstones provides very interesting assumptions concerning their affiliation to a certain lithotype. The scanty siltstone samples from the Orsha and Rudnya formations, available in our pilot collection, represent siltstones or close (in terms of the clastic material dimension) fine-grained (probably, significantly quartz-rich) sandstones. In the $(Na_2O + K_2O)$–$(Al_2O_3 + TiO_2 + Fe_2O_3^* + MnO)/SiO_2$ and $(Na_2O + K_2O)/Al_2O_3$–$(Al_2O_3 + TiO_2 + Fe_2O_3^* + MnO)/SiO_2$ diagrams, their data points fall into the fields of quartz, feldspar–quartz, and arkosic sandstones (Figs. 5a, 5b). At the same time, they differ from the Vendian siltstones by increased content of SiO_2 (79.5...87.8%, maximum 93.9%, sample Bo-1489); decreased content of TiO_2 (0.01–0.19%), Al_2O_3 (4.0–10.7%, 2.5% in sample Bo-1489), and $Fe_2O_3^*$ (0.76–2.4%); and comparable content of total alkalis (2.5–5.5%, 0.15% in sample Bo-1489). Therefore, these samples can be attested as normo-, super-, and hypersilites (HM = 0.04–0.14),

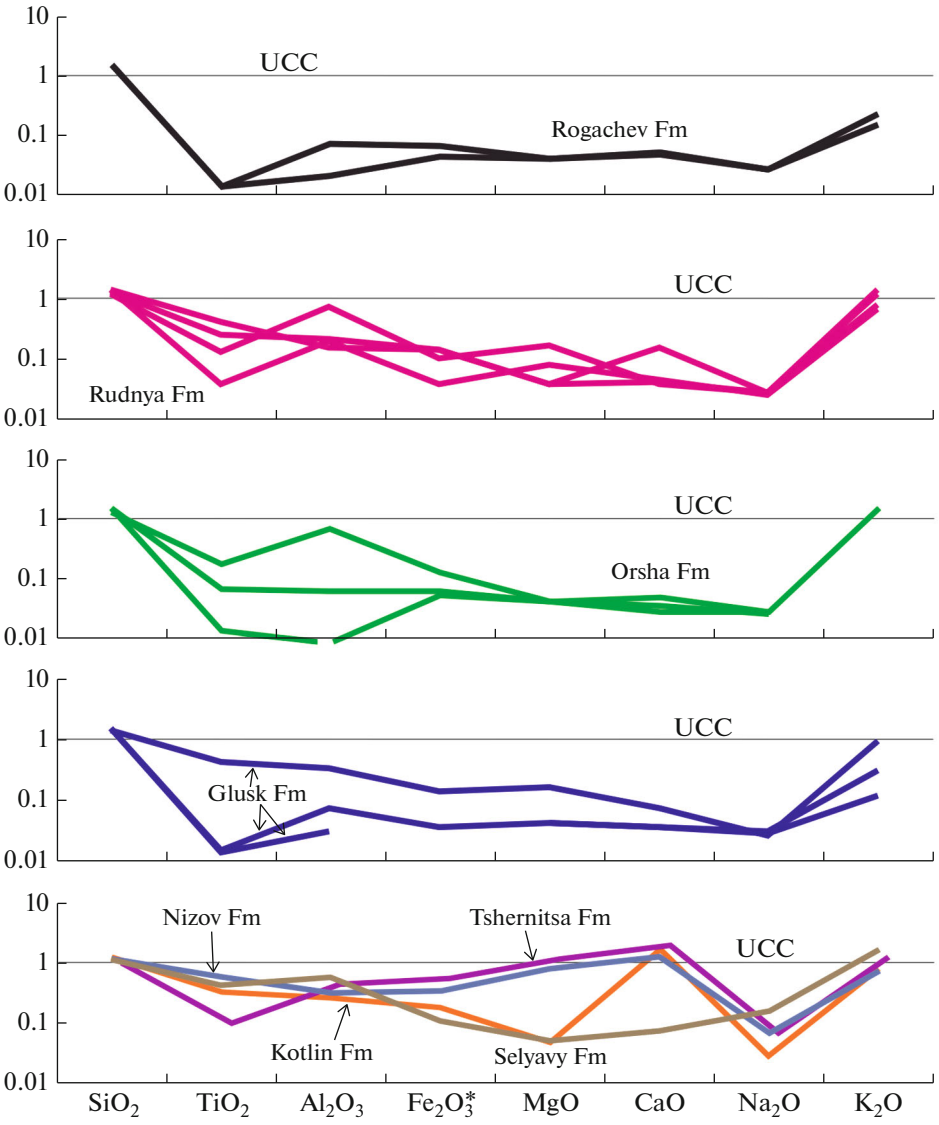

Fig. 4. The UCC-normalized distribution of major oxides in the Riphean and Vendian sandstones.

including the alkaline varieties. Siltstones of the Orsha and Rudnya formations have TM and IM values, similar to those in the feldspar–quartz sandstones of cluster 2 (Fig. 5c).

The Riphean siltstones are characterized by a significant prevalence of K_2O over Na_2O and, accordingly, low AM values (0.02–0.04). However, as in the case of SiO_2, Al_2O_3, and alkali metal concentrations, sample Bo-1489 differs slightly from the remaining siltstones (AM = 1.4). Such values are typical more for sandstones, whereas mudstones have a stable AM value not exceeding 1 ± 0.1, according to (Yudovich and Ketris, 2000). Hence, sample Bo-1489 represents not siltstone but fine-grained sandstone. Moreover, the data point of sample Bo-1489 falls into the field of Fe-sandstones in the $\log(SiO_2/Al_2O_3)$–$\log(Fe_2O_3^*/K_2O)$ diagram; data points of the remaining Riphean siltstones, into the field of subarkoses (Fig. 2c).

In the $(Na_2O + K_2O)/Al_2O_3$–$(Fe_2O_3^* + MnO + MgO)/SiO_2$ diagram (Yudovich and Ketris, 2000), data points of Upper Riphean siltstones and sample Bo-1489 occur in field I (sandstone) or do not fall into any field (Fig. 5d), because they are marked by high low FM (0.01–0.03) but high NAM values. This can be caused by the presence of not only Kfs, but also illite cement and/or appreciable muscovite. For example, in the K_2O/Al_2O_3–Ga/Rb diagram (Roy and Roser, 2013), they fall into the field typical for mudstones dominated by illite (Fig. 5e), but slightly away from the Vendian siltstones. In the K_2O–Al_2O_3 diagram (Van de Kamp, 2016), their data points deviate

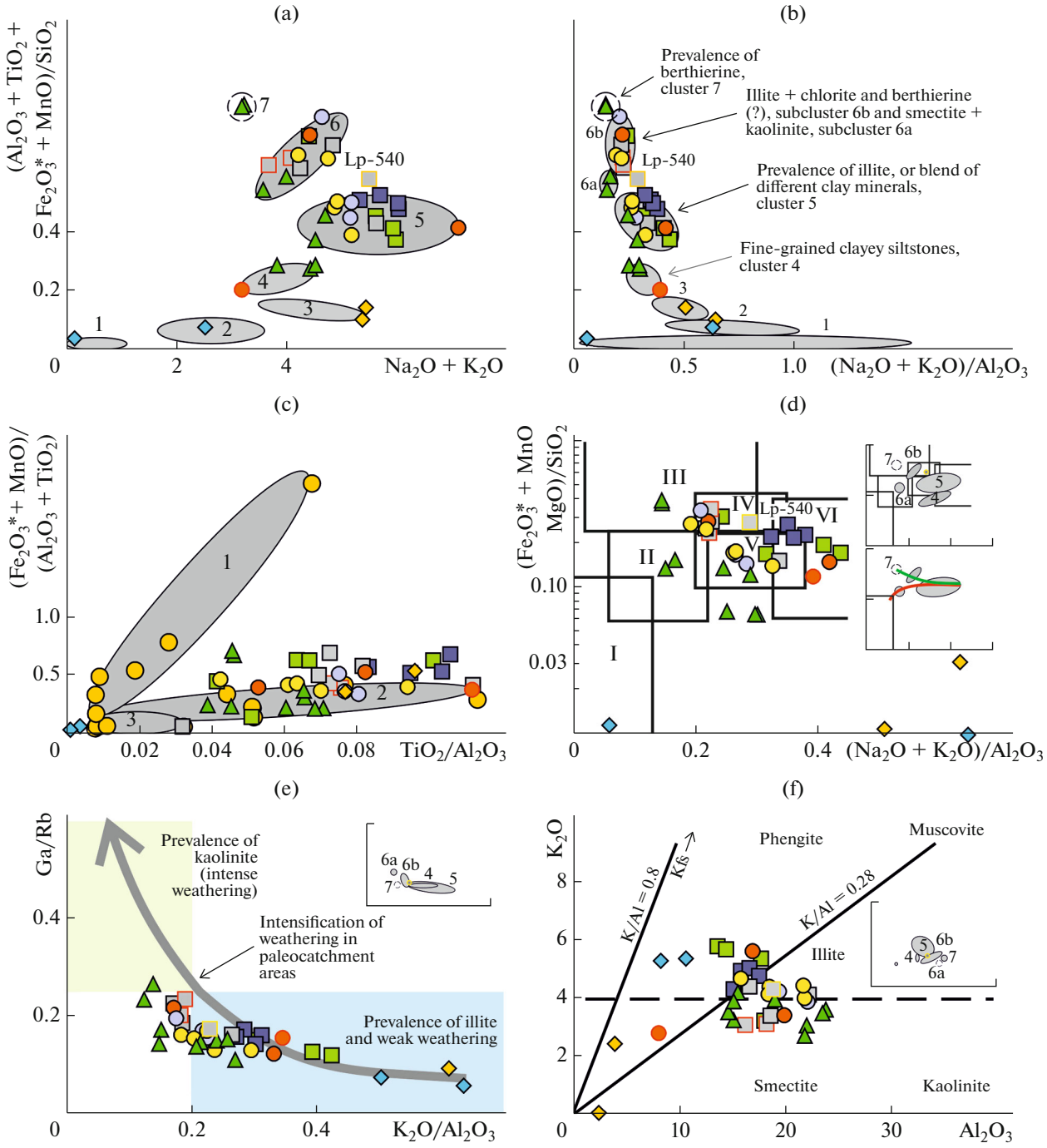

Fig. 5. Position of data points of mudstones and siltstones on diagrams $(Na_2O + K_2O)$–$(Al_2O_3 + TiO_2 + Fe_2O_3^* + MnO)/SiO_2$ (a), $(Na_2O + K_2O)/Al_2O_3$–$(Al_2O_3 + TiO_2 + Fe_2O_3^* + MnO)/SiO_2$ (b), TiO_2/Al_2O_3–$(Fe_2O_3^* + MnO)/(Al_2O_3 + TiO_2)$ (c), $(Na_2O + K_2O)/Al_2O_3$–$(Fe_2O_3^* + MnO + MgO)/SiO_2$ (Yudovich and Ketris, 2000) (d), K_2O/Al_2O_3–Ga/Rb (Roy and Roser, 2013) (e), and K_2O–Al_2O_3 (Van de Kamp, 2016) (f). Legend as in Fig. 2. Insets in (Figs. 2d–2f) show clusters of Vendian siltstones and mudstones (see the text). (d) Fields of claystones: (I) kaolinite; (II) dominated by smectite (kaolinite and illite are subordinate); (III) dominated by chlorite (Fe-illite can occur as admixture); (IV) dominated by illite; (V) standard three-component ("chlorite + smectite + illite") system; (VI) dominated by illite with some finely ground Kfs. Green line in the inset indicates the trend of rock enrichment with smectite, chlorite, iron hydroxides, and berthierine; red line, the trend of rock enrichment with smectite, mixed-layer minerals, and kaolinite.

from the Kfs line toward the illite–muscovite line (Fig. 5f).

Application of the main module diagrams for Vendian siltstones allows us to identify four additional clusters. However, unlike the sandstone clusters, they are not expressed in the diagrams with IM and TM (Fig. 5c). According to these characteristics, Vendian siltstones are highly similar or more ferruginous, relative to the coeval oligomictic and arkosic sandstones. This feature is generally very typical for claystones(!) but not siltstones.

Rocks of cluster 4 (number of samples, $n = 4$) are attested as miosilites (Kotlin Formation) and pseudomiosilites, e.g., Nizov siltstone with the carbonate cement, sample Bo-685, HM 0.21–0.29, NAM 0.25–0.39, ($Na_2O + K_2O$) 3.2–4.6%, and the SiO_2 content varies form 60.9% in the carbonatized siltstone to 68.5–69.6% in other varieties. According to (Yudovich and Ketris, 2000), the miosilite subtype of clastolites is usually represented by the transitional sandstone/mudstone varieties (in other words, siltstones) and sometimes fine-grained clayey varieties that are characterized by the association with claystones (*Sistematika* ..., 1998). As in the case of Riphean siltstones, data points of the Kotlin clayey siltstones do not fall into any of the classification fields in the $(Na_2O + K_2O)/Al_2O_3$–$(Fe_2O_3^* + MnO + MgO)/SiO_2$ diagram (Fig. 5d), although they occur near fields V and II that accommodate the data points of other samples from this formation. The Selyavy siltstone falls into field VI, probably, because of low SiO_2 (due to the carbonatization) and SiO_2/Al_2O_3 values , as well as high K_2O content due to the significant amount of Kfs (Fig. 5f). In the $\log(SiO_2/Al_2O_3)$–$\log(Fe_2O_3^*/K_2O)$ diagram, siltstones of this cluster fall into the field of wackes (probably, due to a significant silt admixture?), while the carbonatized Nizov siltstone falls into the field of arkoses (Fig. 3c).

The examination of clusters 5–7, as well as Liozno sample Lp-540 (borehole Lepel 1), located between cluster 5 and subcluster 6b, (Figs. 5a, 5b), unravels several specific features. Based on the HM value, they can be attested as normosiallites, less commonly, supersiallites in the case of cluster 5 (HM 0.38–0.53, SiO_2 55.3–63.3%, Al_2O_3 13.7–19.5%), or hypohydrolyzates as in the case of clusters 6 and 7 (HM 0.55–0.84, SiO_2 42.0–56.0%, Al_2O_3 16.3–23.9%), but cluster 5 differs from other two clusters by increased AM (4.9–7.2% versus 3.2–4.9%). Rocks in clusters 5–7 are characterized by $K_2O > Na_2O$ (K_2O_{aver} 4.2 ± 0.8%, Na_2O_{aver} 0.7 ± 0.4%) and, correspondingly, low AM values (0.03–0.36, average 0.17 ± 0.09). According to (Yudovich and Ketris, 2000), all these features are more typical for *claystones* rather than siltstones. This statement is also supported by the position of data points of the "siltstones" in the $\log(SiO_2/Al_2O_3)$–$\log(Fe_2O_3^*/K_2O)$ diagram, where they fall into the field of shales and Fe-shales (Figc. 3c, 3d). It is noteworthy that in the later works devoted to the geochemistry of phosphorus, e.g., (Yudovich et al., 2020), attestation of samples to "claystones" is based on the following criteria: $SiO_2 \le 65$–67%, $Al_2O_3 \ge 15$%, and AM < 0.5. Almost all samples of the pilot collection, attested as claystones during the visual description and sampling of drill cores, also satisfy these criteria.

After the geochemical attestation of the fine-grained clayey siltstones and mudstones, we can make the following conclusions concerning the mineralogy of the clayey composition of rocks. Cluster 5 includes: (1) alkaline varieties with the clay minerals dominated by illite ($n = 8$) and the regular significant presence of Kfs, because their data points are concentrated in field VI in the $(Na_2O + K_2O)/Al_2O_3$–$(Fe_2O_3^* + MnO + MgO)/SiO_2$ diagram (Fig. 5d) and the corresponding field in the K_2O/Al_2O_3–Ga/Rb diagram (Fig. 5e); they are deviated from the illite–muscovite line toward Kfs in the K_2O–Al_2O_3 diagram (Fig. 5f); (2) rocks of the mixed composition ($n = 6$) lack obvious signs of the prevalence of any clay minerals (illite, smectite, or chlorite) (field V in the $(Na_2O + K_2O)/Al_2O_3$–$(Fe_2O_3^* + MnO + MgO)/SiO_2$) diagram, which probably includes kaolinite, as suggested by the increase of Al_2O_3 (relative to significantly illite-rich varieties), decrease of K_2O/Al_2O_3 (Fig. 5e), and deviation toward the Al_2O_3 axis (Fig. 5f).

The significantly illite-rich varieties are represented by all Lukoml samples and some samples from the Glusk (Bh-383, Bh-611, Bh-701), Liozno (Lp-528), Nizov (Lp-498), and Tshernitsa (Bo-500) formations, where varieties with the mixed composition are represented by samples from the Selyavy (Bo-658, Bo-660), Tshernitsa (Bo-608, Bo-614), and Kotlin (Bo-515, Bo-521) formations. It is noteworthy that many samples from the Lukoml Formation are marked by an increased MgO content (up to 2.3–3.5%). According to (Yudovich and Ketris, 2000), this feature can be related to the presence of Fe–Mg chlorite, sepiolite, palygorskite, magnesite, dolomite, amphiboles, pyroxenes, and vermiculite. The chemical composition of rocks and information presented in (Jewuła et al., 2022) suggest that chlorite and vermiculite (products of the weathering and transformation of the main clastic material) are the most probable agents among the above-mentioned versions. In addition, field VI in the $(Na_2O + K_2O)/Al_2O_3$–$(Fe_2O_3^* + MnO + MgO)/SiO_2$ diagram, which accommodates some data points of cluster 5, includes products of the Precambrian arid weathering crusts (Yudovich and Ketris, 2000).

Cluster 6 is divided into subclusters. Subcluster 6a includes two Kotlin samples (Lp-321 and Lp-329). As clay rocks of cluster 7, these samples are characterized by the minimum (among the Vendian pelitolites) NAM values (<0.2, Fig. 5b) and FM value comparable to that in some samples with the mixed clayey composition (Fig. 5d). At the same time, these samples fall into field II in the $(Na_2O + K_2O)/Al_2O_3$–$(Fe_2O_3^* + MnO + MgO)/SiO_2$ diagram and along the Al_2O_3 axis in the K_2O–Al_2O_3 diagram (Fig. 5f). They also correspond to the field of kaolinite-dominated varieties in the K_2O/Al_2O_3–Ga/Rb diagram (Fig. 5e). All features mentioned above suggest that subcluster 6a is dominated by smectites and kaolinite.

The rock composition in subcluster 6b ($n = 6$) differs from the counterpart in cluster 5 by higher FM and lower NAM values. Their data points fall into fields III and IV in the $(Na_2O + K_2O)/Al_2O_3$–$(Fe_2O_3^* + MnO + MgO)/SiO_2$ diagram, suggesting the prevalence of chlorite and the presence of illite. This subcluster includes almost all Liozno samples (including the carbonatized varieties with CaO 4.8–10.8%, MgO up to 4.1%, and LOI about 10–11%. This subcluster also includes claystones from the Glusk (Bh-672), Nizov (Bh-675), Tshernitsa (Lp-410, Lp-419), and Selyavy (Bo-661) formations. However, if we take into consideration the data presented in (Jewuła et al., 2022), according to which the chlorite content is low in the Volyn and Redkino mudstones, the increased FM value should be attributed to the presence of not only chlorite, but also berthierine (kaolinite–serpentine), hematite, and goethite. The latter fact can also be suggested by the sufficiently high (for the sample set under consideration) LOI values reaching 15.5–17% in samples Bo-672 (Glusk Formation) and Bo-675 (Nizov Formations), relative to increased $Fe_2O_3^*$ concentrations (11.6–12.7%).

The remaining two Kotlin siltstone samples (Lp-321, Lp-329) combined in cluster 7 are characterized by the highest HM values (0.55 and 0.59) and the lowest AM, FM, and KM values (Fig. 5) among the Vendian fine-grained rocks. However, as in the case of subcluster 6b, we assume that samples Lp-321 and Lp-329 contain berthierine, and increased FM indicates its predominance among clay minerals.

If the major oxides are UCC-normalized, the Riphean siltstones differ significantly from the Vendian fine-grained rocks. The Riphean rocks are characterized by lower contents of Al (0.2...0.7 UCC), Ti (<0.6 UCC), and total Fe (<0.4 UCC) (0.01*n* UCC in siltstones of the Rudnya Formation) (Figs. 6a, 6b). The distribution of major oxides in the Vendian rocks is highly similar—SiO_2 and Al_2O_3 concentrations are close to those in the UCC (1...1.5) or slightly lower except for the Nizov sample Bo-685 (0.6 UCC). The contents of other components are as follows: TiO_2 ~1.5...2.7 UCC, MgO 0.6...1.8 UCC, K_2O 1...2 UCC, and $Na_2O < 0.5$ (more often <0.2 UCC). The $Fe_2O_3^*$ variation is more distinct: from 0.6 UCC in the Nizov sample Bo-685 to 3.1...3.3 UCC (commonly 1.2...3.1 UCC) in the probably berthierine-rich Kotlin samples. Most significant are variations of MnO (from 0.14...2.2 to 2.9...9.8, maximums in the carbonatized varieties), CaO (0.05...3.1, maximums in the same samples), and P_2O_5 (up 1...3.2...18.5 (!!) UCC with maximum in the Nizov sample Bo-6850.

It should be emphasized that the CaO content in Vendian siltstones and mudstones correlate with P_2O_5 (correlation coefficient, $r_{0.05(CaO-P_2O_5)} = 0.76$). However, the correlation becomes geochemically insignificant ($r_{0.05(CaO-P_2O_5)} = 0.21$) if we exclude samples Bo-732, Bo-711, Bo-608, and Lp-360, which are marked by anomalous P_2O_5 concentrations (>0.48%)—according to (Yudovich et al., 2020), the Clarke P_2O_5 value for pelites is 0.140 ± 0.005%—as well as the Nizov sample Bo-685. The latter sample is also characterized by high concentrations of CaO, MnO, and MgO. Probably, a notable portion of P in rocks with the above-Clarke P_2O_5 concentrations is included in the accessory apatite, whereas the varieties with near- and below-Clarke concentrations can show the correlation of P with Fe ($r_{0.05} = 0.41$) and Mg ($r_{0.05} = 0.62$). Such correlations indicate presence of P in the absorbed form in smectites, chlorite, or iron hydroxides (Yudovich et al., 2020).

Thus, almost all Riphean siltstones in our pilot collection along with some samples taken from the Kotlin and Nizov formations represent real siltstones, whereas the remaining Vendian "siltstones" should be attested as claystones. In the case of Riphean samples, we believe that the rocks visually defined as siltstones are coarse-grained siltstones or fine-grained sandstones enriched with quartz or feldspar–quartz, since they are similar in many ways to counterparts in terms of geochemistry. In our opinion, all facts mentioned above makes it possible to consider the Middle Riphean siltstones and sandstones together in further research.

With regard to Vendian siltstones, we can assume that they are fine-grained clay varieties, judging by their geochemical features that are closer to those of other Vendian fine-grained rocks identified by us as mudstones based on various criteria. It is known that the clay fraction is the main concentrator of several trace elements (*Geochemistry ...*, 2003; Taylor and McLennan, 1985; and others), and claystones are considered the most correct proxies of provenance composition over vast paleocatchment areas (Cullers, 1988; Cullers et al., 1987, 1988; *Interpretatsiya ...*, 2001; Taylor and McLennan, 1985; and others). Therefore, we are somehow "free" in further recon-

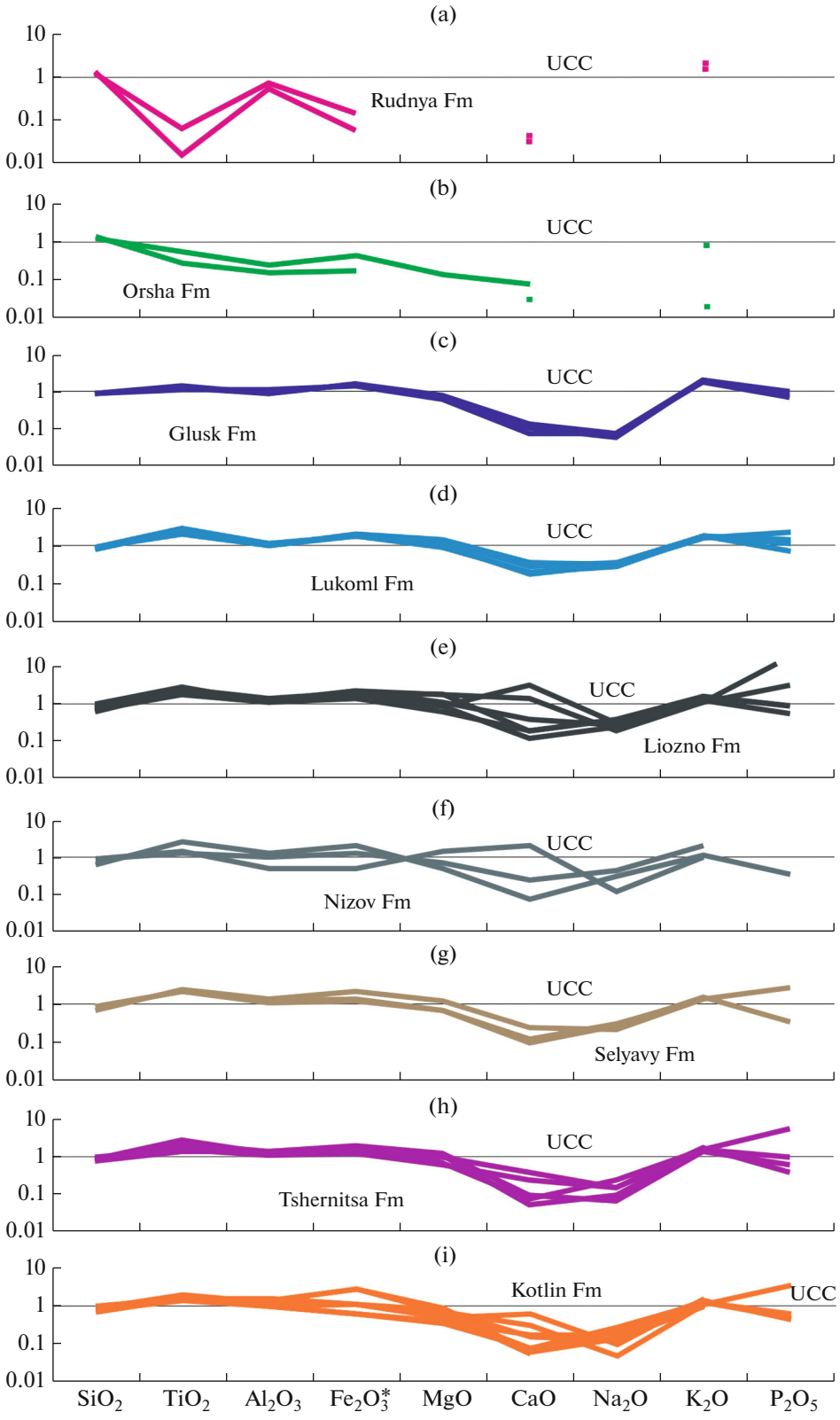

Fig. 6. The UCC-normalized distribution of major oxides in the Riphean and Vendian mudstones and siltstones.

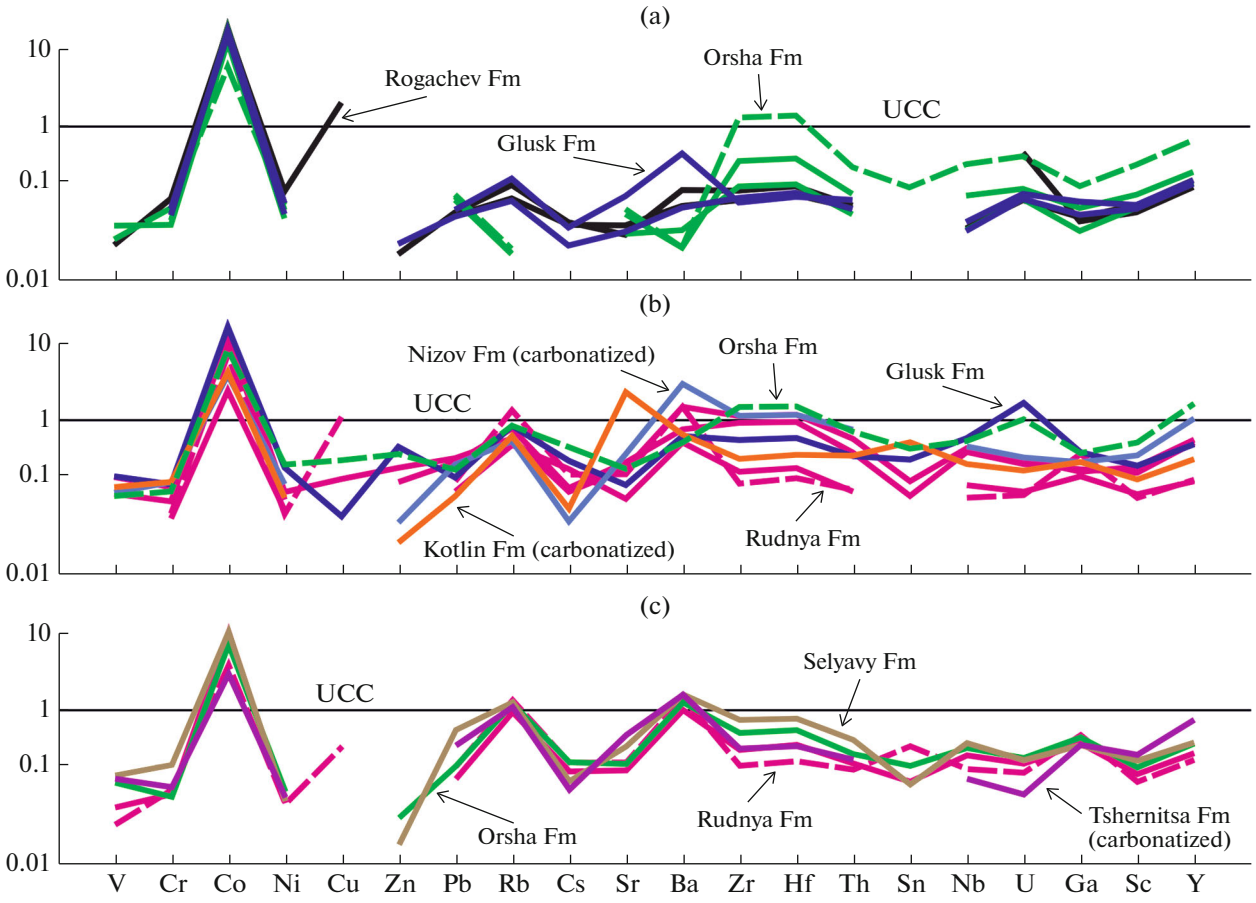

Fig. 7. The UCC-normalized distribution of trace elements (except REE) in the Riphean siltstones (dashed lines) and the Riphean and Vendian sandstones (solid lines). (a) Assumed quartz-rich, (b) feldspar–quartz, and (c) arkosic varieties.

structions of the paleoclimate and provenance; i.e., we can accomplish the reconstructions without any conditionality, as in the case of siltstones.

It should be emphasized that the sample set of fine-grained rocks includes some samples with a significant proportion of CaO (and sometimes MgO and LOI). In addition, some samples in our collection contain a notable amount of P_2O_5, probably, associated with accessory minerals. These samples should be used with caution in future studies or excluded from consideration. In general, the variable content of clay fraction, as well as the presence of carbonate and phosphate admixtures, encourage us to use a geochemical technique, such as enrichment factor, $EF = (X/Al)_{sample}/(X/Al)_{reference\ object}$, where X is the concentration of element (Van der Weijden, 2002), for which EF is calculated), during the examination of the distribution of trace elements in Vendian mudstones and siltstones. As reference object for the mudstones and fine-grained clayey siltstones, we shall use PAAS (Taylor and McLennan, 1985) with correction for REE, Sc, and Y according to (Pourmand et al., 2012) and for Nb according to (Barth et al., 2016).

DISTRIBUTION OF TRACE ELEMENTS

Riphean Siltstones and Riphean–Vendian sandstones

All hyper-, super-, and normosilites represented by the Upper Riphean–Vendian sandstones and Middle Riphean siltstones, assigned to clusters 1, 2, and 3 (quartz-rich, oligomictic, and arkosic varieties, respectively) in the lithochemical certification demonstrate a similar distribution pattern of trace elements (Fig. 7), regardless of the assumed lithotype (sandstone/siltstone) or cement (carbonatized/non-carbonatized) type. This fact once again confirms the assumption that they should be considered together.

Sandstones and siltstones are characterized by the enrichment in Co (2.4...19.3 UCC), but depletion (commonly <0.1 UCC) in other siderophile elements (V, Cr, Ni), sulfophile elements (Pb, in rare cases Cu and Zn), and some lithophile elements (Cs, Sr, Sn, Ga, and Sc). At the same time, several peculiarities in the element distribution that can be explained by changes in the mineralogical composition: (1) variation in the content of Rb, Nb, and Ba from <0.1 UCC in the assumed quartz sandstones to 1.0 UCC and slightly more in arkoses, which is attributed to increase

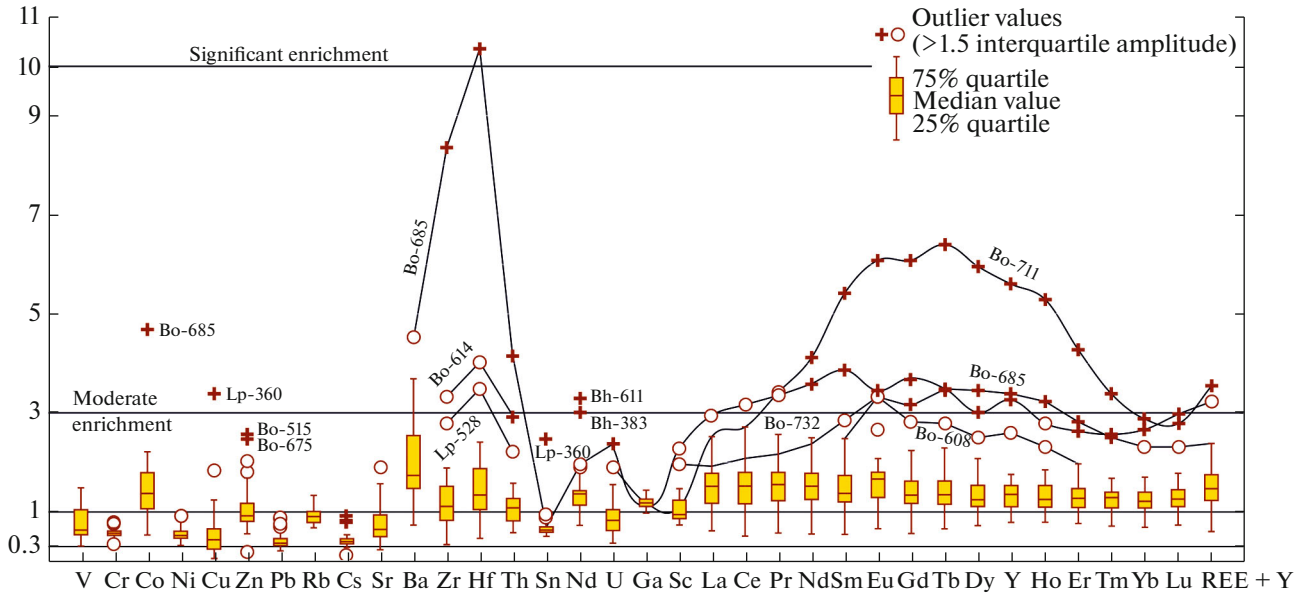

Fig. 8. Values of EF for trace elements in Vendian mudstones and siltstones (sample set). The "moderate–significant enrichment" gradation is adopted from (Tribovillard et al., 2006).

in the proportion of alkaline feldspars in them; (2) variation in the concentration of Zr, Hf, Th, and Y that does not depend on the age and assumed petrotype, and, probably, reflects the variable amount of accessory minerals in rocks. We believe that the enrichment with Cu, Zn, and Sn in some samples is related to the presence of pyrite (probably, even pyrite cement), and the enrichment with U is related to redox conditions in the "bottom water–sediment" system.

Vendian Mudstones and Fine-Grained Clayey Siltstones

When considering the enrichment factors (EF) of Vendian fine-grained clastic rocks (Fig. 8), we should first note the common features and the presence of some "anomalies" in the sample set. The anomalies mainly correspond to anomalous and extreme values, whereas the distribution of trace elements is not always symmetrical. Therefore, we will often use hereafter the term "median value," which is more appropriate for such distributions. All samples are characterized by the depletion in Cr (EF = 0.34...0.78), Ni (0.32...1.08), Pb (0.21...0.88), and Cs (0.12...0.94), as well as insignificant enrichment in Ga (<1.5). In general, the EF values of the listed elements for all Vendian rocks are comparable.

Samples Bo-732 and Bo-711 (Liozno Formation) mentioned in the previous section, as well as Bo-608 (Tshernitsa Formation) with high P_2O_5 concentrations are enriched to a variable extent relative to PAAS, but very significantly relative to other claystone samples (Fig. 8) with MREE and HREE. According to the classification in (Tostevin et al., 2016), rare earth elements are divided into three groups: LREE (La, Ce, Pr, Nd); MREE (Sm, Eu, Gd, Tb, Dy); and HREE (Ho, Er, Tm, Yb, Lu) + Y. At the same time, sample Bo-711, characterized by the maximum P_2O_5 content (~2.8%), is also enriched with LREE, Sc, and U. However, sample Lp-360 (Kotlin Formation, P_2O_5 0.52%), which lacks the above features, represents an exception moderately enriched with Cu (EF_{Cu} = 3.4) and Sn (EF_{Sn} = 2.5), probably, due to the presence of impurities, e.g., sulfides (pyrite, chalcopyrite, or less common minerals). The Nizov sample Bo-685, characterized by high concentrations of CaO, MnO, and MgO, is distinguished by EF = 2.5...5 for Co, Ba, Th, U, Nb, and REE, and EF > 8 (!) for Zr and Hf. The sample set, from which all the listed samples are excluded (Fig. 9, Table 3), are discussed below.

Also noteworthy are samples of the fine-grained clastic rocks Bo-614 (Tshernitsa Formation) and Lp-528 (Liozno Formation), which are 2.2–4 times enriched (compared to PAAS) with Zr, Hf, and Th, as well as samples Bh-611 and Bh-383 (Glusk Formation) containing a notable amount of Nb and samples Bo-675 (Nizov Formation) and Bo-515 (Kotlin Formation) enriched with Zn (Fig. 8). The presence of Zr, Hf, and Th is most probably related to accessory minerals, since these elements have positive significant correlation with Ti (Table 3). The content of Nb (and, very expectedly, Rb) shows direct correlation with the concentration of K (Kfs and illite).

The fine-grained clastic rocks of the Glusk Formation are characterized by the lowest median (<0.5) EF_V values (Fig. 9). They are also marked by a distinct (though insignificant) enrichment with Rb and mod-

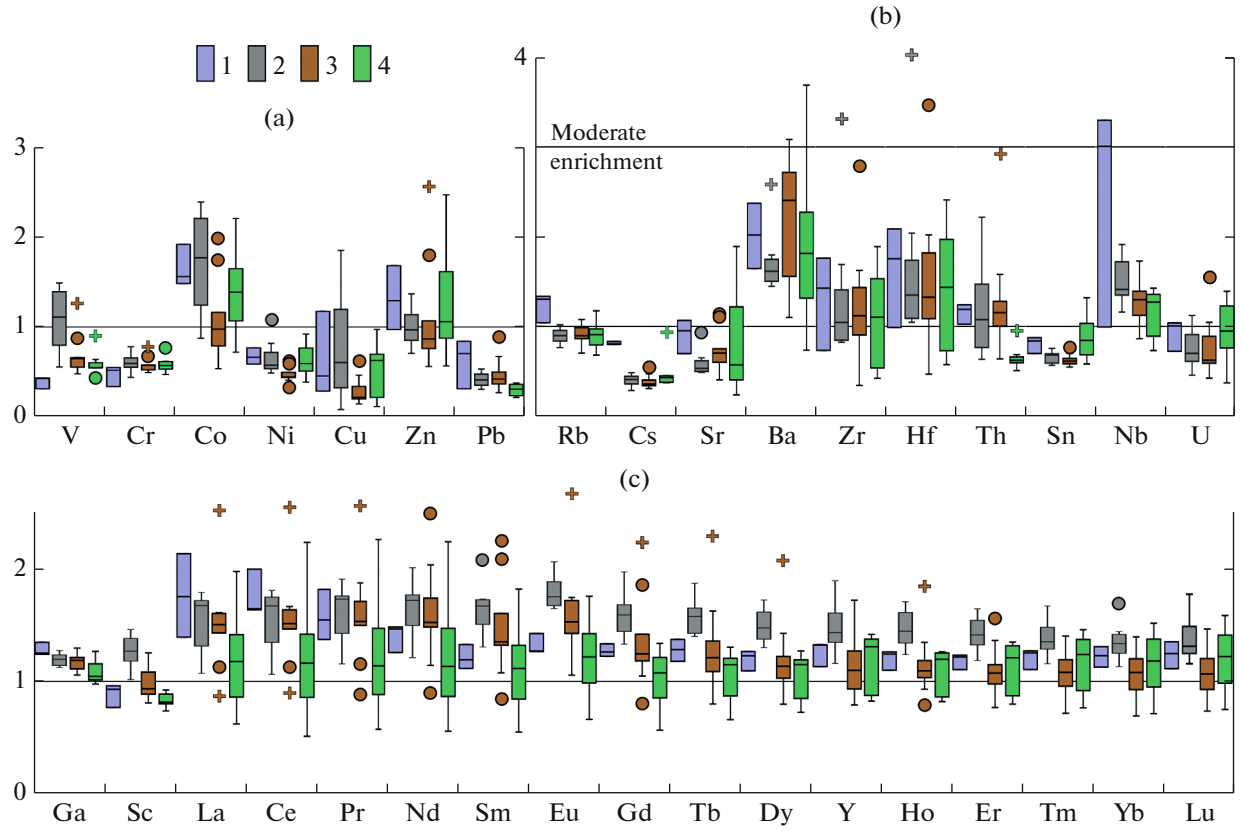

Fig. 9. Values of EF for trace elements in the Vendian mudstones and siltstones (sample set without samples enriched with CaO and P_2O_5, see the text). (1) Glusk Formation ($n = 3$); (2) Lukom and Liozno formations ($n = 8$); (3) Redkino stratigraphic level ($n = 9$); (4) Kotlin Formation ($n = 8$).

erate enrichment with Nd. Based on indicators, such as EF_{Zr} and EF_{Hf}, rocks of this formation are characterized by the highest median values (average 1.5 times, while the value is close to 1 for other formations). Rocks of the Volyn Group are slightly enriched in V and Sc (EF up to 1.5). They are also distinguished by high (usually, not only median) EF values for MREE and HREE (not so distinct for Yb and Lu) and Y (Fig. 9c) than other fine-grained Vendian rocks in our pilot collection. Moreover, in relation to Ga, Sc, LREE, and MREE, one can see a trend of median values in the Volyn Group rocks decreasing upward the section, whereas this trend is disrupted for HREE and Y by an increase of median values in the Kotlin samples. The LREEs were likely transported to claystones mainly by the Ti-containing minerals, whereas the MREE, Y, and HREE were transported not only by phosphates, but also by some Fe- and Mg-containing clay minerals, as may be evidenced by the presence of geochemically significant correlations (Table 3).

Rocks of the Redkino regional stage are characterized, firstly, by the lowest EF values for Co, Ni, Cu, Cs, and Sn among the fine-grained Vendian clastic rocks (except for some samples) and, secondly, by the highest median EF values. The Kotlin clayey siltstones and mudstones distinguished by a wide range of EF values (from differently depleted to slightly and moderately enriched) for Co, Zn, Sr, Ba, Zr, Hf, Sn, U, and REE.

Nature of the Vendian and Riphean Rocks

The nature of the lithogenic/petrogenic material composing the sandstones and fine-grained clastic rock samples in our collection can be deciphered by several methods. Firstly, as shown in (Yudovich and Ketris, 2000), if the correlation is positive between TM and IM for a particular sample set, but negative between NAM and HM, then this sample set is represented by the petrogenic rocks that underwent only one sedimentation cycle (weathering → transport → burial) and vice versa. Indeed, both for Riphean siltstones and sandstones ($n = 13$, $r_{TM–IM} = 0.38$, $r_{NAM–HM}$ is -0.31), as well as Vendian mudstones and clay siltstones ($n = 34$, $r_{TM–IM} = 0.13$, $r_{NAM–HM}$ -0.60), positive and negative correlations are observed between these modules. However, in our opinion, they satisfy the criterion of Y.E. Yudovich and M.P. Ketris only formally, since only one of the listed correlations

Table 3. Geochemically significant ($r \geq r_{0.05}$) correlations of different components and modules for Vendian mudstones and clayey siltstones ($n = 28$)

	SiO_2	TiO_2	Al_2O_3	$Fe_2O_3^*$	MnO	MgO	Na_2O	K_2O	P_2O_5	LOI	HM	FM	TM	IM	NAM	AM	KM
SiO_2		–0.41	–0.76	–0.81		–0.57				–0.67	–0.97	–0.88		–0.48	0.54		0.55
TiO_2	–0.41						0.56						0.85			0.59	
Al_2O_3	–0.76							–0.49		0.63	0.80	0.47	–0.37		–0.84		–0.81
$Fe_2O_3^*$	–0.81					0.65			0.42		0.83	0.98		0.87			
MnO																	0.42
MgO	–0.57			0.65					0.55		0.52	0.72		0.60			
Na_2O		0.56											0.63			0.94	
K_2O			–0.49							–0.55					0.84		0.89
P_2O_5				0.42		0.55						0.46		0.46			
LOI	–0.67		0.63					–0.55			0.62				–0.68		–0.67
HM	–0.97		0.80	0.83		0.52				0.62		0.89		0.46	–0.62		–0.62
FM	–0.88		0.47	0.98		0.72			0.46		0.89			0.78			
TM		0.85	–0.37				0.63								0.37	0.60	
IM	–0.48			0.87		0.60			0.46		0.46	0.78					
NAM	0.54		–0.84					0.84		–0.68	–0.62		0.37				0.96
AM		0.59					0.94						0.60				
KM	0.55		–0.81		0.42			0.89		–0.67	–0.62				0.96		
V	–0.65	0.64	0.42	0.50					0.42	0.49	0.61	0.54	0.41				–0.40
Cr	–0.62		0.77					–0.39		0.55	0.61				–0.57		–0.63
Co										–0.45							
Ni	–0.50		0.61	0.39		0.51					0.55	0.48	–0.38		–0.49		–0.44
Cu									0.48					0.47			
Zn										0.61							
Pb	–0.42									0.58							
Rb							–0.50	0.41					–0.43			–0.67	
Sr				–0.48								–0.45		–0.52			
Zr		0.39											0.51				
Hf		0.39											0.51				
Th		0.45															
Sn	–0.68		0.63	0.44						0.66	0.67	0.47			–0.51		–0.42
Nb					0.46			0.42						0.45	0.41		0.48
Cs		–0.38	0.44				–0.53						–0.54			–0.52	
U														–0.40			
Ga	–0.88		0.86	0.66		0.43				0.56	0.92	0.74			–0.69		–0.66
Sc	–0.77	0.80	0.52	0.67		0.61			0.49		0.74	0.72	0.50	0.42		0.38	–0.42
LREE		0.47															
MREE	–0.55	0.64				0.49			0.64		0.50	0.46	0.38				
Y	–0.41	0.55				0.55			0.57		0.39	0.42					
HREE	–0.48	0.66		0.40		0.44			0.46		0.48	0.48	0.46			0.38	–0.38

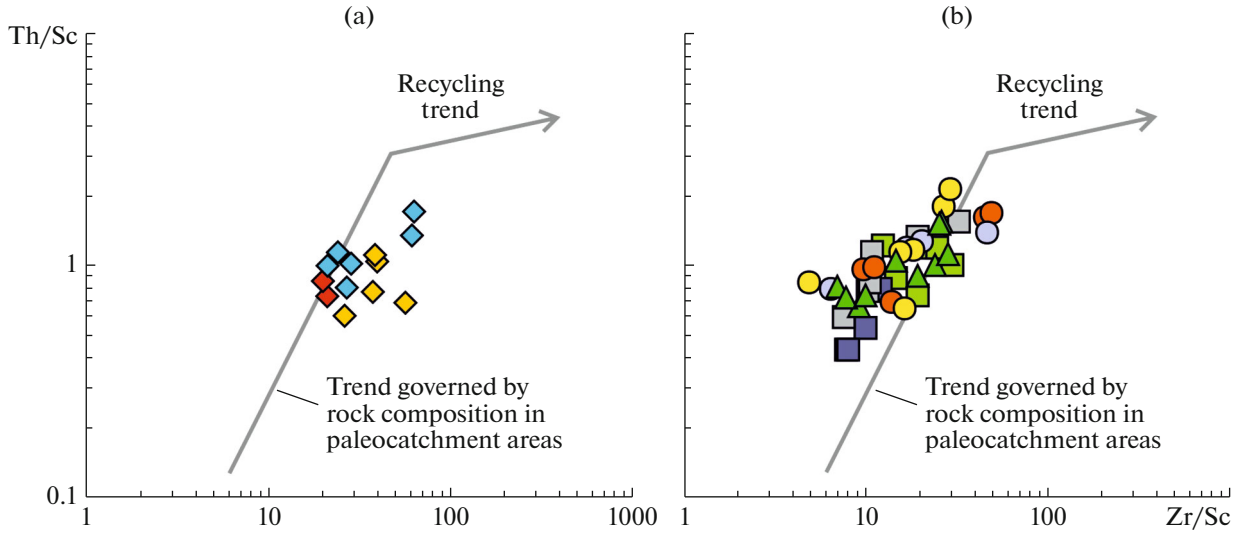

Fig. 10. Distribution of data points of Riphean (a) and Vendian (b) sandstones, siltstones, and mudstones on the Zr/Sc–Th/Sc diagram (McLennan et al., 1993). Legend as in Fig. 2.

($r_{NAM–HM}$ –0.60) is statistically significant for the Vendian fine-grained formations.

Secondly, according to (McLennan et al., 1993), the ratio of Zr, Sc, and Th in the fine-grained clastic rocks also allows us to judge the nature of the material therein. The criteria presented in the above work suggest that the composition of all samples is dominated by the material of the first sedimentation cycle (Fig. 10), which does not contradict the data for mudstones of the Volyn and Valdai groups in the western EEP (Jewuła et al., 2022). The exception is provided by several samples of the Middle Riphean (Rudnya and Orsha) sandstones and siltstones—their data points on the Zr/Sc–Th/Sc diagram clearly deviate from the variation trend of the provenance rock composition, which can be interpreted in favor of the presence of lithogenic components therein.

CONCLUSIONS

Analysis of the position of data points of clastic rock samples in our pilot collection in various diagrams, their geochemical attestation according to the method in (Yudovich and Ketris, 2000), and examination of the distribution pattern of trace elements, allow us to draw the following conclusions.

Rocks, visually defined as sandstones during the description of drill core and sampling, actually represent the petrogenic quartz-rich and feldspar–quartz varieties and arkoses with different content of the lithogenic admixture and various (including carbonate) types of cement. The presence of lithogenic admixture is especially typical for the Rudnya and Orsha rocks. At the same time, Upper Riphean (coarse-grained?) siltstones of the Rudnya and Rogachev formations are very similar in geochemistry to the coeval sandstones. Therefore, we can analyze them together in further research. We did not find any significant regularity in the composition of different-age sandstones. The recorded regularities are mainly associated, apparently, with variations in the content of Kfs, accessory minerals, and sulfides in them.

The Vendian rocks, visually identified as siltstones during the description of drill core and sampling, contain a significant amount of clay and represent the compositionally heterogeneous (fine-grained?) clayey siltstones and mudstones dominated by illite, illite-berthierine, berthierine, kaolinite, and smectite. Precisely the presence of berthierine and iron hydroxides (and not only chlorite) was responsible for the increase of FM in several samples. Some samples of the Vendian fine-grained clastic rocks show a notable amount of sulfides, carbonate component, and/or accessory apatite (e.g., samples with above-Clarke (>0.48%) content of P_2O_5, which is the carrier of U and REE.

The petrogenic nature of material in the majority of clastic rock samples in the studied pilot collection suggests the following point: conclusions regarding the main factors for the formation of primary sediments, based on diverse techniques and approaches in the practice of lithogeochemical studies, are sufficiently correct.

The revealed lithogeochemical features of Middle Riphean–Vendian sandstones, siltstones, and mudstones govern both possibilities and some limitations for their application in further geochemical studies. For example, the presence of carbonate cement and berthierine constricts the possibility of using such samples with diagrams based on the major oxides. The presence of accessory apatite constricts the application of indicator ratios including certain lanthanides in the formulas. At the same time, the significant

amount of clay components in "siltstones" and their petrogenic nature dismisses several restrictions. Taking into account the geochemical peculiarities of rock formations revealed by the comparison of samples with the UCC and PAAS, indicators using V, Cr, Ni, Rb, Zr, Hf, Th, Sc, and some REE will be most suitable for the provenance reconstructions, since they demonstrate the minimum/moderate dispersion in the sample set. In other words, variation in their concentrations is related primarily to the provenance composition but not to peculiarities of the depositional environment.

ACKNOWLEDGMENTS

During the manuscript preparation, fragments proposed by O.F. Kuzmenkova and A.G. Laptsevich were taken into account and added to the text with corresponding references. The authors are grateful to G.D. Streltsova and S.S. Mankevich for the help in selecting drill core samples, as well as to anonymous reviewers whose comments and suggestions made it possible to improve the style and presentation of the material. Illustrations for the article were prepared by N.S. Glushkova.

FUNDING

This work was accomplished under state tasks of Geological Institute, Moscow (project no. FMMG-2023-0004, lithogeochemical investigation), Institute of Precambrian Geology and Geochronology, St. Petersburg (FMUW-2021-0003, collection of samples, their primary description and preparation for analytical studies) and Zavaritsky Institute of Geology and Geochemistry, Yekaterinburg (FUMZ-2023-0008, interpretation of lithochemical data based on approaches developed under the current project).

CONFLICT OF INTEREST

The authors of this work declare that they have no conflicts of interest.

REFERENCES

Barth, M.G., McDonough, W.F., and Rudnick, R.L., Tracking the budget of Nb and Ta in the continental crust, *Chem. Geol.*, 2000, vol. 165, pp. 197–213.

Bordon, V.E., *Geokhimiya i metallonosnost' osadochnogo chekhla Belorussii* (Geochemistry and Metal Potential of the Sedimentary Cover in Belarus), Minsk: Nauka Tekhn., 1977.

Cullers, R.L., Mineralogical and chemical changes of soil and stream sediment formed by intense weathering of the Danberg Granite, Georgia, USA, *Lithos*, 1988, vol. 21, pp. 301–314.

Cullers, R.L., Barrett, T., Carlson, R., and Robinson, B., Rare-earth element and mineralogic changes in Holocene soil and stream sediment: a case study in the Wet Mountains, Colorado, USA, *Chem. Geol.*, 1987, vol. 63, pp. 275–297.

Cullers, R.L., Basu, A., and Suttner, L.J., Geochemical signature of provenance in sand-size material in soils and stream sediments near the Tobacco Root Batholith, Montana, USA, *Chem. Geol.*, 1988, vol. 70, pp. 335–348.

Geochemistry of Sediments and Sedimentary Rocks: Evolutionary Considerations to Mineral Deposit-Forming Environments, Lentz, D.R., Ed., St. Jones: Geol. Ass. Canada, 2003.

Geologiya Belarusi (Geology of Belarus), Makhnach, A.S., Garetskii, R.G., and Matveev, A.V., Eds., Minsk: Inst. Geol. Nauk Belarusi, 2001.

Golubkova, E.Yu., Kuzmenkova, O.F., and Kushim, E.A., et al., Distribution of microfossils in the Vendian deposits of the Orsha Depression of the East European Platform, Belarus, *Strat. Geol. Correl.*, 2021, vol. 29, no. 6, pp. 627–640.

Golubkova, E.Yu., Kuzmenkova, O.F., Laptsevich, A.G., et al., Paleontological characteristics of the Upper Vendian–Lower Cambrian sediments in the section of the North Polotsk Borehole of the East European Platform, Belarus, *Strat. Geol. Correl.*, 2022, no. 6, pp. 457–474

Herron, M.M., Geochemical classification of terrigenous sands and shales from core or log data, *J. Sedim. Petrol.*, 1988, vol. 58, pp. 820–829.

Interpretatsiya geokhimicheskikh dannykh (Interpretation of the Geochemical Data), Sklyarov, E.V., Ed., Moscow: Intermet Inzhin., 2001.

Jewula, K., Środoń, J., Kędzior, A., et al., Sedimentary, climatic, and provenance controls of mineral and chemical composition of the Ediacaran and Cambrian mudstones from the East European Craton, *Precambr Res.*, 2022, vol. 381, p. 106850.

Kuzmenkova, O.F., Laptsevich, A.G., Streltsova, G.D., and Minenkova, T.M., Riphean and Vendian in the conjugation zone of the Orshanskaya Depth and the Zlobin Saddle (Bykhovskaya parametric borehole), in *Problemy geologii Belarusi v smezhnykh territorii* (Problems of Geology in Belarus and Adjacent Regions), Minsk: SroiMediaProekt, 2018, pp. 101–105.

Kuzmenkova, O.F., Laptsevich, A.G., and Glaz, N.V., Issue of the Middle Riphean Bortniki Formation in Belarus, in *Etapy formirovaniya i razvitiya proterozoiskoi zemnoi kory: stratigrafiya, metamorfizm, magmatizm, geodinamika* (Stages of the Formation and Evolution of the Earth's Proterozoic Crust: Stratigraphy, Metamorphism, Magmatism, and Geodynamics), St. Petersburg: Svoe Izd-vo, 2019, pp. 122–124.

Kuzmenkova, O.F., Laptsevich, A.G., Kuznetsov, A.B., et al., Important issues of the Riphean–Vendian Stratigraphy in the Volyn–Orsha paleoaulacogen in the western East European Platform, in *Etapy formirovaniya i razvitiya proterozoiskoi zemnoi kory: stratigrafiya, metamorfizm, magmatizm, geodinamika* (Stages of the Formation and Evolution of the Earth's Proterozoic Crust: Stratigraphy, Metamorphism, Magmatism, and Geodynamics), St. Petersburg: Svoe Izdvo, 2019, pp. 125–127.

Laptsevich, A.G., Golubkova, E.Yu., Kuzmenkova, O.F., et al., The Upper Vendian Kotlin Horizon in Belarus: Lithological differentiation and biostratigraphic substantiation, *Litasfera*, 2023, no. 1(58), pp. 17–25.

Makhnach, A.S., Stratigraphic scheme of the Upper Precambrian in Belarus, in *Geologicheskoe stroenie i perspektivy neftegazonosnosti BSSR* (The Geological Structure and Pe-

troleum Potential of the BSSR), Moscow: Nedra, 1966, pp. 210–236.

Makhnach, A.S., Veretennikov, N.V., and Shkuratov, V.I., Stratigraphy of Upper Proterzozoic rocks in Belarus, *Izv. AN SSSR. Ser. Geol.*, 1975, no. 3, pp. 90–103.

Makhnach, A.S., Veretennikov, N.V., Shkuratov, V.I., and Bordon, V.E., *Rifei i vend Belorussii* (The Riphean and Vendian in Belarus), Minsk: Nauka Tekhn., 1976.

Makhnach, A.S., Ol'khovik, E.T., and Bordon, V.E., *Geokhimiya venda Belorussii* (The Vendian Geochemistry in Belarus), Minsk: Nauka Tekhn., 1982.

Maslov, A.V., Podkovyrov, V.N., and Graunov, O.V., Provenances of fine-grained alumosiliciclastic material for the Vendian and Early Cambrian sedimentary rocks of the west of the East European Plate: some lithogeochemical constraints, *Strat. Geol. Correl.*, 2024, vol. 32, no. 1, pp. 1–20.

McLennan, S.M., Geochemistry and Mineralogy of Rare Earth Elements, *Rev. Miner. Geochem.*, 1989, vol. 21, pp. 169–200.

McLennan, S.M., Taylor, S.R., McCulloch, M.T., and Maynard, J.B., Geochemical and Nd–Sr isotopic composition of deep-sea turbidites: crustal evolution and plate tectonic associations, *Geochim. Cosmochim. Acta*, 1990, vol. 54, pp. 2015–2050.

McLennan, S.M., Hemming, S.R., McDaniel, D.K., and Hanson, G.N., Geochemical approaches to sedimentation, provenance and tectonics, in *Processes Controlling the Composition of Clastic Sediments*, Johnsson, M.J. and Basu, A., Eds., *Geol. Soc. Am. Spec. Pap.*,1993, no. 284, pp. 21–40.

Paleogeografiya i litologiya venda i kembriya zapada Vostochno-Evropeiskoi platformy (The Vendian–Cambrian Paleogeography and Lithology in the Western East European Platform), Keller, B.M. and Rozanov, A.Yu., Ed., Moscow: Nauka, 1980.

Paszkowski, M., Budzyn, B., Mazur, S., et al., Detrital zircon U–Pb and Hf constraints on provenance and timing of deposition of the Mesoproterozoic to Cambrian sedimentary cover of the East European Craton, Belarus, *Precambr. Res.*, 2019, vol. 331, p. 105352.

Pettijohn, F.J., Potter, P.E., and Siever, R., *Sand and Sandstone*, New York: Springer, 1976.

Pourmand, A., Dauphas, N., and Ireland, T.J., A novel extraction chromatography and MC-ICP-MS technique for rapid analysis of REE, Sc and Y: Revising CI-chondrite and Post-Archean Australian Shale (PAAS) abundances, *Chem. Geol.*, 2012, vol. 291, pp. 38–54.

Roy, D.K. and Roser, B.P., Climatic control on the composition of Carboniferous–Permian Gondwana sediments, Khalaspir basin, Bangladesh, *Gondwana Res.*, 2013, vol. 23, pp. 1163–1171.

Rudnick, R.L. and Gao, S., Composition of the continental crust, in *The Crust*, Rudnick, R.L., Holland, H.D., and Turekian, K.K., Eds., Oxford: Elsevier Pergamon, 2003, pp. 1–64 (Treatise on Geochemistry, vol. 3.)

Sistematika i klassifikatsiya osadochnykh porod i ikh analogov (Systematics and Classification of Sedimentary Rocks and Their Analogs), Shvanov, V.N., Ed., St. Petersburg: Nedra, 1998.

Środoń, J., Gerdes, A., Kramers, J., and Bojanowski, M.J., Age constraints of the Sturtian glaciation on western Baltica based on U-Pb and Ar-Ar dating of the Lapichi Svita, *Precambrian Res.*, 2022, vol. 371, p. 106595.

Stratigraficheskie skhemy dokembriiskikh i fanerozoiskikh otlozhenii Belarusi. (Stratigraphic Schemes of Precambrian and Phanerozic Deposits in Belarus), Minsk: BelNIGRI, 2010, Explanatory Note.

Strel'tsova, G.D., Laptsevich, A.G., and Kuzmenkova, O.F., *Riphean deposits in eastern Belarus, Aktual'nye problemy nauk o Zemle: issledovaniya transgranichnykh region (Important Problems in Earth Sciences: Study of the Transboundary Region)*, Brest: BGU, 2023, pp. 200–203.

Taylor, S.R. and McLennan, S.M., *The Continental Crust: Its Composition and Evolution*, Oxford: Blackwell, 1985.

Tostevin, R., Shields, G.A., Tarbuck, G.M., et al., Effective use of cerium anomalies as a redox proxy in carbonate-dominated marine settings, *Chem. Geol.*, 2016, vol. 438, pp. 146–162.

Tribovillard, N., Algeo, T.J., Lyons, T., and Riboulleau, A., Trace metals as paleoredox and paleoproductivity proxies: An update, *Chem. Geol.*, 2006, vol. 232, pp. 12–32.

Van de Kamp, P.C., Potassium distribution and metasomatism in pelites and schists: how and when? Relation to post-depositional events, *J. Sediment. Res.*, 2016, vol. 86, pp. 683–711.

Van der Weijden, C.H., Pitfalls of normalization of marine geochemical data using a common divisor, *Mar. Geol.*, 2002, vol. 184, pp. 167–187.

Yudovich, Ya.E., Blast from the past, *Vestn. Inst. Geol. Komi Nauchn. Tsentra Ural. Otd. RAN*, 2007, no. 5, pp. 25–33.

Yudovich, Ya.E. and Ketris, M.P., *Osnovy litokhimii* (Fundamentals of Lithochemistry), St. Petersburg: Nauka, 2000.

Yudovich, Ya.E., Ketris, M.P., and Rybina, N.V., *Geokhimiya fosfora* (Geochemistry of Phosphiorus), Syktyvkar: IG Komi NTs UrO RAN, 2020.

Zaitseva T.S., Kuzmenkova O.F., Kuznetsov A.B., et al. The U–Th–Pb Age of Detrital Zircon from the Riphean Sandstones of the Volyn–Orsha Paleotrough, Belarus, *Strat. Geol. Correl.* 2023, vol. 31, no. 5, pp. 390–409.

Translated by D. Sakya